

# SE(3)-Equivariant Attention Networks for Shape Reconstruction in Function Space

Evangelos Chatzipantazis<sup>\*1</sup>, Stefanos Pertigkiozoglou<sup>\*1</sup>, Edgar Dobriban<sup>2</sup>, and Kostas Daniilidis<sup>1</sup>

<sup>1</sup> Department of Computer and Information Science, University of Pennsylvania

<sup>2</sup> Department of Statistics and Data Science, University of Pennsylvania

vaghat@seas.upenn.edu, pstefano@seas.upenn.edu,  
dobriban@wharton.upenn.edu, kostas@cis.upenn.edu

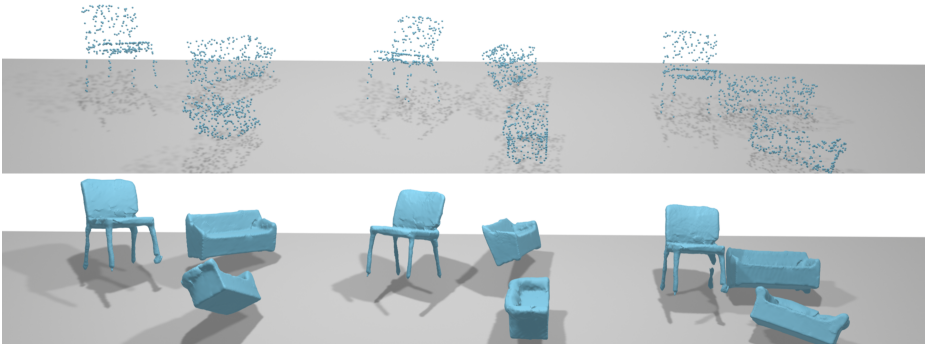


Fig. 1: (Above): Sparse point clouds individually SE(3)-transformed to form a single scene of nine objects. (Below): Our equivariant reconstruction. The network is agnostic to the number, position and orientation of the objects and is trained only on single objects in canonical pose.

**Abstract.** We propose the first SE(3)-equivariant coordinate-based network for learning occupancy fields from point clouds. In contrast to previous shape reconstruction methods that align the input to a regular grid, we operate directly on the irregular, unoriented point cloud. We leverage attention mechanisms in order to preserve the set structure (permutation equivariance and variable length) of the input. At the same time, attention layers enable local shape modelling, a crucial property for scalability to large scenes. In contrast to architectures that create a global signature for the shape, we operate on local tokens. Given an unoriented, sparse, noisy point cloud as input, we produce equivariant features for each point. These serve as keys and values for the subsequent equivariant cross-attention blocks that parametrize the occupancy field. By querying an arbitrary point in space, we predict its occupancy score. We show

<sup>\*</sup> Equal contribution

that our method outperforms previous  $SO(3)$ -equivariant methods, as well as non-equivariant methods trained on  $SO(3)$ -augmented datasets. More importantly, local modelling together with  $SE(3)$ -equivariance create an ideal setting for  $SE(3)$  scene reconstruction. We show that by training only on single objects and without any pre-segmentation, we can reconstruct a novel scene with single-object performance.

**Keywords:**  $SE(3)$ -equivariance, equivariant implicit reconstruction, equivariant occupancy field, equivariant attention, local shape modelling, product group transformations, scene reconstruction

## 1 Introduction

With the advent of range sensors in robotics and in medical applications, research in shape reconstruction from point clouds has been seen increasing activity [4]. The performance of classical optimization methods tends to degrade when point clouds become sparser, noisier, unoriented, or untextured. Deep learning methods have been proven useful to encode shape priors, and solve the reconstruction problem end to end [43]. Various 3D representations have been proposed, depending on memory scalability and on amenability to encode and process arbitrary topologies and complex geometries. With such desiderata in mind, deep learning methods that operate on meshes [51,24], voxels [43], and point clouds [42] have been built. Each has strengths and limitations. While the canonical structure of voxels leads to easy manipulation, shape resolution is limited by memory. On the other hand, while meshes can guarantee watertight reconstructions, they only handle a predefined topology. Point clouds are lightweight in terms of memory, but they discard topology. Recently proposed deep learning methods represent the geometry via a learned occupancy map, or a signed distance function. In particular, the seminal work of [35] inspired many follow-up works [39,9,23,45]. Such representations can encode arbitrary topologies with an effectively infinite resolution.

According to Kendall, “Shape is the geometry of an object modulo position, orientation, and scale” [28]. While intensive research in the field [36,40,37] has led to increasingly better results, very few of these methods incorporate symmetries as an inductive bias for learning. Most translation-equivariant reconstruction methods build on the convolutional occupancy network [40], while the only  $SO(3)$ -equivariant architecture for reconstruction, to our knowledge, is the Vector Neurons method [14]. We propose the first  $SE(3)$ -equivariant coordinate-based network for shape reconstruction. Motivated by the  $SE(3)$ -transformer [20], we design a two-level network that first extracts local features from the point cloud using equivariant self-attention. Second, a cross-attentional occupancy network takes the coordinates of a point with its local feature vector as a query, and the outputs of the encoder as keys and values, and outputs the occupancy function value at the query point.

In contrast to [15], the output representation of our encoder captures specific locations in space, thus facilitating the compositionality of scenes. Even unique

objects usually consist of smaller primitive parts, whose subsets are subsequently composed to form large collections of objects. Local shape modelling exploits this composability to generalize to unseen objects and scenes of arbitrarily placed objects. Our equivariant fully attention-based design extracts local features in the first part of the architecture, on tokens that are points. Encoding local shape priors and exploiting compositionality to avoid retraining on every possible scene combination is distinct from typical encoder-decoder architectures that extract a global signature description of the input. Scenes consisting of multiple objects (Fig. 1) can be reconstructed without retraining even if each object is individually rotated and translated. Moreover, our method differs from state of the art methods such as [40,46], because it works directly on the irregular point cloud without any alignment via interpolation functions [40], or voxelization by average pooling [46].

Finally, SE(3)-equivariance not only facilitates equivariant reconstructions by design, but it also benefits training by constraining the space of allowed reconstructions. Our experiments show that we achieve comparable or better performance than state of the art networks, with much fewer parameters and fewer training epochs.

Our contributions can be summarized as follows:

- We have built the first SE(3)-equivariant **coordinate-based** and **end-to-end attentional** network for shape reconstruction from sparse point clouds.
- Our network encodes shapes locally and does not need to assume that objects are centered. It is, thus, fully SE(3)—and not just SO(3)—equivariant. Moreover, it can reconstruct scenes where objects are transformed individually without needing to be trained on scenes, and without segmentation.
- Experimentally, we outperform other equivariant networks (Vector Neurons) and standard networks (Occupancy Networks, Convolutional Occupancy Networks) trained with augmentations.

## 2 Related Work

In this section, we present previous work on surface reconstruction from input point clouds. We focus on methods that reconstruct the surface of an object by using a function defined in 3D space, such as the occupancy function or the signed distance function (SDF). In these methods, the final surface can be extracted by taking the 0-level set of the corresponding function.

For oriented point clouds (with known normal vectors), the occupancy function or the SDF can be constructed by classical methods such as the Moving Least Squares method [1], and via Screened Poisson Surface Reconstruction [27]. These methods do not require any prior learning, but they tend to fail in the presence of noise. If the normal vectors are not known, their performance depends heavily on the normal estimation algorithm used as a preprocessing step. To surpass such limitations, [35,10] proposed to learn the occupancy function for each input point cloud. Similarly, [39] proposed to learn the SDF of the object

surface, conditioned on a latent code that can be inferred from a sparse set of SDF values.

A limitation of the above methods is that they use a global feature vector—or code—to represent the whole object or scene. This global feature does not allow the decomposition of an object into smaller parts, which may reduce the generalization ability of the method to unseen inputs. More recent methods exploit the similarities between local patches of different objects by learning either a combination of local and global features [23,17], or only local ones [26,5,49]. The composition of such local features allows to reconstruct scenes containing a variety of objects. To define the local neighborhoods for which the local features are extracted, [26,5,49] voxelize the space into a regular grid and learn a feature representation for each voxel. This regular grid creates neighborhoods that do not depend on the geometry of the object. This may limit the ability of the model to reconstruct novel compositions of objects. In our work, we avoid the use of such static neighborhoods by using local attention layers [3] that dynamically change the attention weights of each point to its neighbors. Attention layers were popularized in natural language processing with the introduction of the transformer architecture [50], and were later applied in computer vision tasks such as image classification [16,54]. Specifically for point cloud processing tasks, [38] used both local and global attention for object detection, and [55] used a transformer for point cloud completion.

The reconstruction of an object’s shape should be independent of the coordinate system. Additionally, when the input is a point cloud, the reconstruction should also be invariant to the ordering of the given points. As a result, we want the shape reconstruction to be invariant to permutations of the points, and to also be equivariant to rotations and translations. Most of the methods presented above are invariant to permutations of the input points, but do not ensure equivariance to translations and rotations.

There is a large body of work on incorporating known symmetries into the learning process. A first major success of such methods can be traced back to [21,30] with the use of convolutional layers to build translation-equivariant networks. More recent works extend this idea to discrete [13] and continuous [53] rotationally invariant architectures. These methods have also been applied beyond Euclidean domains, to spheres [18], graphs [34] and general manifolds [12]. Additionally, for transformer architectures, [20] propose an SE(3)-equivariant transformer by using the results of Tensor Field Networks [48]; [44] proposed a framework for constructing linear self-attention layers that are equivariant to arbitrary discrete groups.

Operating on point clouds, an SE(3)-equivariant network [8] performs pose estimation and classification using SE(3) convolutions. For the problem of surface reconstruction from point clouds, Convolutional Occupancy Networks [40] and later methods [31,46] use convolutional layers to achieve translation-equivariance. Finally, [15] propose Vector Neurons, which converts general neural network architectures to SO(3)-equivariant ones. [15] apply vector neurons to SO(3)-equivariant surface reconstruction from point clouds. To our knowledge, this is

the only method that uses an  $\text{SO}(3)$ -equivariant model to learn the occupancy function for surface reconstruction.

### 3 Method

#### 3.1 SE(3) Equivariant Reconstruction

Shape reconstruction should be independent of the coordinate system used, including the position of the origin and the orientation of the coordinate axes. One way to capture this geometric consistency is via  $\text{SE}(3)$ -equivariance, which can be formulated using group theory.

Given a map  $f$  from an input space  $\mathcal{X}$  to an output space  $\mathcal{Y}$ — $f : \mathcal{X} \rightarrow \mathcal{Y}$ —and a group  $G$  acting on  $\mathcal{X}, \mathcal{Y}$  via  $\cdot, *$ , respectively, the map  $f$  is called  $(G, \cdot, *)$ -equivariant if  $g * f(x) = f(g \cdot x)$ , for all  $g \in G$  and  $x \in \mathcal{X}$ . The principle of equivariance is fundamental, lying at the heart of—among other natural sciences—physics under the name of “Einstein’s general covariance”. We will assume some basic familiarity with abstract group theory and representation theory, and defer a more extensive discussion to the Appendix.

Groups can act on numerous mathematical objects. Of interest to us are the linear group actions on vector spaces, i.e., *group representations*. Formally, given a group  $G$  and a vector space  $V$ , a group representation of  $G$  on  $V$  is the pair  $(V, \rho)$  where  $\rho : G \rightarrow \text{GL}(V)$  is a group homomorphism to the invertible linear transformations over  $V$ . According to the Peter-Weyl theorem, linear representations of compact groups like  $\text{SO}(3)$  can be decomposed into a direct sum of finite-dimensional, unitary, irreducible sub-representations.

In particular, if  $\rho$  is a representation of  $\text{SO}(3)$  on a finite dimensional vector space  $V$ , then after choosing a basis, we can write  $\rho(r) = \mathbf{Q}^T [\bigoplus_l \mathbf{D}_l(r)] \mathbf{Q}$ , for all  $r \in \text{SO}(3)$ , where  $\mathbf{Q}$  is a change of basis matrix, and for any  $l \in \mathbb{N}$ ,  $\mathbf{D}_l$  is the  $l$ -th irreducible representation of  $\text{SO}(3)$ , called a *Wigner D-matrix*. The invariant subspace  $V_l$  of  $V$  acted on by  $\mathbf{D}_l$  has dimension  $(2l + 1)$ , and its elements are called *type- $l$*  vectors. A type-0 vector is a scalar staying invariant to rotations, a type-1 vector rotates as a Euclidean 3D vector, type-2 vectors are traceless symmetric matrices, etc.

Consider the group of proper rigid transformations, isomorphic to  $\text{SE}(3) \cong (\mathbb{R}^3, +) \times \text{SO}(3)$ , and denote its elements by  $(t, r)$ . The standard group action of  $\text{SE}(3)$  on 3D vectors  $\vec{x}$  is  $(t, r) \cdot \vec{x} = R_r \vec{x} + T_t$ , where  $T_t \in \mathbb{R}^3$  and  $R_r \in \text{SO}(3)$ . The group can also act on functions defined on a homogeneous space of the group via the induced representation. For a function  $f : \mathbb{R}^3 \rightarrow \mathbb{R}^n$  the left regular representation  $\mathcal{L}$  of  $\text{SE}(3)$  induced by the  $n$ -dimensional representation  $\rho$  of  $\text{SO}(3)$  is the transformation law defined as

$$\begin{aligned} \mathcal{L}_{(t,r)}[f](\vec{x}) &= \rho(r)f(R_{r^{-1}}(\vec{x} + T_{t^{-1}})) \\ &= \rho(r)f(R_r^{-1}(\vec{x} - T_t)), \text{ forall } (r, t) \in \text{SE}(3). \end{aligned} \tag{1}$$

Then  $f$  is called a  $\rho$ -field. In particular, if  $\rho$  is the  $l$ -th irreducible representation of  $\text{SO}(3)$ , we call  $f$  a *type- $l$  field*. An example of a type-0 (scalar) field, which

is of interest in this paper, is the occupancy function of a shape. Higher order fields (such as vector and tensor fields) will be discussed later. In deep networks, the difference between stacked channels and those forming a  $\rho$ -field is that the latter are defined by transformation laws, providing a geometrical meaning to the representations.

In the next two sections, we discuss the representation of the input/output fields and the construction of our equivariant pipeline, depicted in Fig. 2.

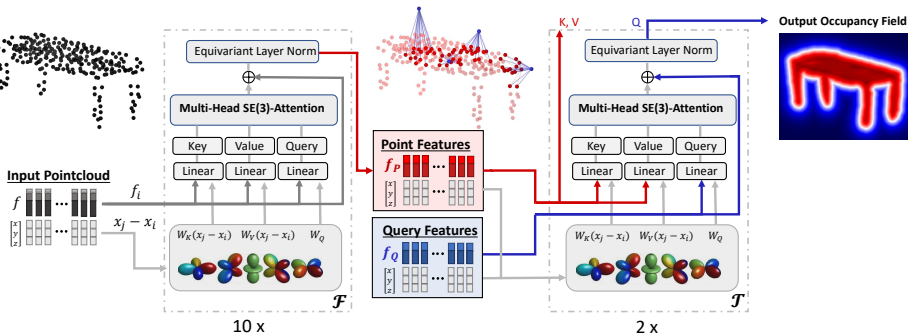


Fig. 2: Our method consists of two networks  $\mathcal{F}$ ,  $\mathcal{T}$ . First, to each point  $\vec{x}_i$  in the point cloud, we assign a simple local feature  $\mathbf{f}_i$  of type-1 (rotating as a vector) which can be the relative position of  $\vec{x}_i$  to the centroid of its local neighborhood. Similarly, to each query point  $\vec{q} \in \mathbb{R}^3$  we assign a local feature  $\mathbf{f}_q$ . Given a point cloud consisting of pairs  $(\vec{x}_i, \mathbf{f}_i)$ , the network  $\mathcal{F}$  applies SE(3)-equivariant attention to assign to each point  $\vec{x}_i$  a learned type-1 feature  $\mathbf{f}_P$ . Finally, given the set of pairs  $(\vec{x}_i, \mathbf{f}_P)$  and the query-feature pair  $(\vec{q}, \mathbf{f}_q)$ , the network  $\mathcal{T}$  applies SE(3)-equivariant cross-attention to output the scalar value of the occupancy function at point  $\vec{q}$ .

### 3.2 Learning the Occupancy Field

Consider an unordered set of 3D points  $\mathcal{P} = \{\vec{x}_i\}_{i=1}^N$ . This point cloud can be oriented (with normal vectors attached to the points) or unoriented. Each point may have a different identity and associated features (e.g., atomic number or part identity of a segmented shape). In the general case, the input consists of positions and optional features  $(\vec{x}_i, \mathbf{f}_i)_{i=1}^N$ . The number  $N$  can vary between point clouds, a property we account for in our design. A point cloud with features can be thought of as a map  $f : \mathbb{R}^3 \rightarrow \mathbb{R}^n$  with  $f(\vec{x}) = \sum_{i=1}^N \mathbf{f}_i \delta(\vec{x} - \vec{x}_i)$ .

We design the architecture of an SE(3)-equivariant operator  $\mathcal{T}$  acting on the input function  $f$  to produce a new function  $o_f : \mathbb{R}^3 \rightarrow [0, 1]$  that describes the occupancy score  $o_f(\vec{q})$  of each position  $\vec{q} \in \mathbb{R}^3$ . Following [35], we parametrize  $\mathcal{T}$  by a coordinate-based neural network. Then, given a function  $f$  on the point cloud, and an arbitrary point  $\vec{q}$  in space, we predict  $\mathcal{T}[f](\vec{q}) = o_f(\vec{q}) \in [0, 1]$ . The

scalar field  $o_f$  approximates the true *occupancy function*  $o^* : \mathbb{R}^3 \rightarrow \{0, 1\}$  whose 0-level set,  $\{\vec{x} \in \mathbb{R}^3 | o^*(\vec{x}) = 0\}$ , encodes the volume occupied by the object and whose boundary encodes the surface of the object. A simultaneous roto-translation of both the point cloud and the query point results in the same true occupancy value. This property is captured by our SE(3)-equivariant network  $\mathcal{T}$ .

While SE(3)-equivariance ensures consistency across coordinate systems, generalization performance is dependent on the features  $\{\mathbf{f}_i, i \in [N]\}$  input to  $\mathcal{T}$ . Even though our method can incorporate external information (e.g., normal vectors or part identity), we focus on unoriented point clouds, without additional features other than the set of position vectors. For this reason, we propose to start from relatively simple hand-designed features and jointly learn more complex features simultaneously with learning the occupancy field. We use an SE(3)-equivariant self-attention operator  $\mathcal{F}$  that, given simple hand-designed features  $\{\mathbf{f}_i, i \in [N]\}$ , produces an equivariant local signature  $\mathbf{f}_P = \{\mathbf{f}_{P_i}, i \in [N]\}$  of the point cloud. This is subsequently used as an input to the occupancy network  $\mathcal{T}$ .

We describe the construction of the features  $\{\mathbf{f}_i, i \in [N]\}$  used as an input to  $\mathcal{F}$ . Given an input point cloud  $\mathcal{P} = \{\vec{x}_i\}_{i=1}^N$ , we first assign to each point  $\vec{x}_i \in \mathcal{P}$  a neighborhood  $\mathcal{N}(\vec{x}_i)$ , containing its  $k$  nearest neighbors. Then, we attach to it the feature  $\mathbf{f}_i$  of its relative position from the neighborhood’s centroid. This is a type-1 vector, transforming according to the standard representation of SO(3). In other words, a roto-translation  $(R_r, T_t)$  of the point cloud will transform the pairs to  $(R_r\vec{x}_i + T_t, R_r\mathbf{f}_i)$ . Both the type of the feature and the transformation-invariance of the neighborhood plays a role in this transformation. The input to the network can be thought of as a type-1 field on the homogeneous space  $\mathbb{R}^3 \cong \text{SE}(3)/\text{SO}(3)$ , of the form  $f(\vec{x}) = \sum_{i=1}^N \mathbf{f}_i \delta(\vec{x} - \vec{x}_i)$ . Then, the transformation law above corresponds to the induced representation  $\mathcal{L}_{(t,r)}[f](\vec{x}) = R_r f(R_r^{-1}(\vec{x} - T_t)) = \sum_{i=1}^N (R_r \mathbf{f}_i) \delta((R_r^{-1}(\vec{x} - T_t) - \vec{x}_i))$ .

Instead of the Dirac point masses  $\delta(\cdot)$  we will concatenate the points  $\vec{x}_i$  row-wise into a matrix  $X = [\vec{x}_i^T]_{i=1, \dots, N} \in \mathbb{R}^{N \times 3}$ . Then, the action of roto-translation on the point cloud is defined as

$$\mathcal{L}_{(t,r)}[X] = X R_r^T + \oplus_N T_t^T, \quad \text{for all } (t, r) \in \text{SE}(3) \quad (2)$$

where  $\oplus_N$  denotes row-wise concatenation  $N$  times.

The output of the first equivariant network  $\mathcal{F}$  is another feature map  $\mathbf{f}_P = \{\mathbf{f}_{P_i}, i \in [N]\}$  on the point cloud. Since the input is a *type-1* field and the network  $\mathcal{F}$  is SE(3)-equivariant, the output field could potentially have any type, or even be a concatenation of fields of various types. Here we will use type-1 vectors as the output  $\mathbf{f}_P$ .

Similarly, we need to design features  $\mathbf{f}_q$  for each query point  $\vec{q}$  that we input to  $\mathcal{T}$ . We first assign to  $\vec{q}$  the neighborhood of its closest point in the point cloud, i.e.,  $\mathcal{N}(\vec{q}) = \mathcal{N}(\arg \min_{\vec{x} \in \mathcal{P}} \|\vec{q} - \vec{x}\|_2)$ . Details on ties are deferred to the Appendix. We then construct the same type-1 feature  $\mathbf{f}_q$  as before, namely,  $\mathbf{f}_q$  is the position vector relative to the centroid of the neighborhood  $\mathcal{N}(\vec{q})$ . The

learned features  $\{(\vec{x}_i, \mathbf{f}_{P_i})\}_{i=1}^N$  on the point cloud, and the query-feature pair  $(\vec{q}, \mathbf{f}_{\vec{q}})$ , are the inputs to the second equivariant network  $\mathcal{T}$ .

The output of the second network corresponds to the occupancy value of the point  $\vec{q}$ . It is selected as a type-0 field; thus, a simultaneous roto-translation of the object and the query  $q$  results in an invariant prediction, as required.

In Fig. 3 we depict the query field (type-1) and the output occupancy field (type-0). Observe the transformation law of both fields as the point cloud is roto-translated in space. Equivariance of  $\mathcal{T}$  is equivalent to the diagram being commutative.

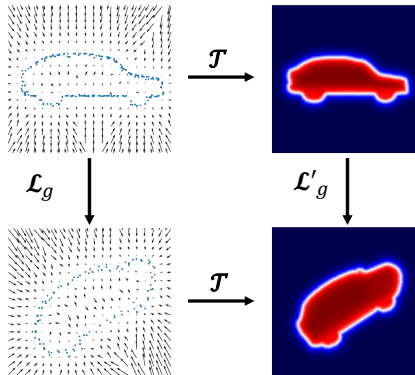


Fig. 3: (Left): Input query field (type-1) and its rotation, (Right): output occupancy field (type-0) and its rotation. Here  $\mathcal{L}_g$  describes the action on both the query field (the vector field on the left) and the point cloud type-1 field  $\mathbf{f}_P$  described in the main text (not shown here). The action  $\mathcal{L}_g$  has the form from (1), while  $\mathcal{T}$  being equivariant is equivalent to the diagram being commutative, i.e.,  $\mathcal{L}_g \circ \mathcal{T} = \mathcal{T} \circ \mathcal{L}_g$ .

### 3.3 Equivariant Attention for Shape Reconstruction

We propose to construct our networks  $\mathcal{F}, \mathcal{T}$  as a composition of equivariant attention modules.

Given  $N_{\text{out}}$  query tokens  $Q_i \in \mathbb{R}^{d_Q}$  and  $N_{\text{in}}$  key-value pairs  $K \in \mathbb{R}^{N_{\text{in}} \times d_Q}$ ,  $V \in \mathbb{R}^{N_{\text{in}} \times d_V}$ , an attention module can be described by the formula (with subscripts indexing rows)

$$A(Q_i, K, V) = V^T \text{softmax}(KQ_i) = \sum_{j=1}^{N_{\text{in}}} \frac{\exp(Q_i^T K_j)}{\underbrace{\sum_{j'=1}^{N_{\text{in}}} \exp(Q_i^T K_{j'})}_{\alpha(Q_i, K_j)}} V_j, \quad i \in [N_{\text{out}}].$$

For each query token  $Q_i$ , the output  $A$  is a linear combination of the values  $V_j$ , modulated by the similarity  $\alpha(Q_i, K_j)$  of the query  $Q_i$  to the corresponding key



$K_j$  as imposed by the attention kernel  $\alpha$ . When all queries, keys and values are functions of the same feature vector, the module is called *self-attention*. When the keys and values are functions of the same feature, but this feature differs from the one in the query, the module is called *cross-attention*. In our setup, in addition to the dependency on the features  $\{\mathbf{f}_i, i \in [N]\}$ , the attention networks depend on the position vectors  $X$  of the points.

We design the first network  $\mathcal{F}$  as a composition of  $L$  self-attention layers, where each of the  $N$  points has a query token with the same functional dependency

$$Q = Q(\vec{x}, \mathbf{f}) = W_Q \mathbf{f}.$$

If  $\vec{x}_j \in \mathcal{N}(\vec{x}_i)$ , we assign to the pair  $(\vec{x}_i, \vec{x}_j)$  a key-value token. The functional form of keys and values is

$$V(\mathbf{f}, \vec{y}, \vec{x}) = W_V(\vec{y} - \vec{x})\mathbf{f}, \quad K(\mathbf{f}, \vec{y}, \vec{x}) = W_K(\vec{y} - \vec{x})\mathbf{f}.$$

The attention module at layer  $l \in [L]$  thus is

$$\mathcal{F}_l[f, X](\vec{x}_i) = \sum_{\vec{x}_j \in \mathcal{N}(\vec{x}_i)} \frac{\exp[(W_Q \mathbf{f}_i)^T (W_K(\vec{x}_j - \vec{x}_i) \mathbf{f}_j)]}{\sum_{\vec{x}_j \in \mathcal{N}(\vec{x}_i)} \exp[(W_Q \mathbf{f}_i)^T (W_K(\vec{x}_j - \vec{x}_i) \mathbf{f}_j)]} W_V(\vec{x}_j - \vec{x}_i) \mathbf{f}_j,$$

and  $\mathcal{F} = \mathcal{F}_L \circ \dots \circ \mathcal{F}_2 \circ \mathcal{F}_1$ . Note that  $X$  passes through in all layers.

To ensure SE(3)-equivariance, we constrain  $W_Q$ ,  $W_K$ , and  $W_V$ . As required by the rules of processing induced representations, the attention module takes a  $\rho_{\text{in}}$ -field as the input and produces a  $\rho_{\text{out}}$ -field as the output. These fields consist of various irreducible representations appearing with multiplicities. As discussed in the preliminaries, from the Peter-Weyl theorem, we can decompose the feature vectors as  $\mathbf{f}^{\text{in}} = \bigoplus_l \bigoplus_{m_l} \mathbf{f}_{l, m_l}^{\text{in}}$  and  $\mathbf{f}^{\text{out}} = \bigoplus_k \bigoplus_{n_k} \mathbf{f}_{k, n_k}^{\text{out}}$ , where we selected the standard basis. Each  $\mathbf{f}_{l, m_l}$  is a type- $l$  feature, with  $m_l$  indexing the multiplicity. One way to transform a  $\rho_{\text{in}}$ -field to a  $\rho_{\text{out}}$ -field is to impose the necessary constraints so that each of the three linear layers in the attention module performs this transformation.

Absent any dependency on position,  $W_Q$  has to satisfy the equation  $W_Q \rho_{\text{in}}(r) = \rho_{\text{out}}(r) W_Q$ , for all  $r \in \text{SO}(3)$ . From Schur's lemma, it follows that  $W_Q$  has to be zero between different irreducible types, and contains a single parameter between irreducible representations of the same type. Viewing multiplicities as channels, the solution corresponds to a 1-by-1 convolution.

Even though  $W_Q$  can exchange information only between multiplicities of the same type, the functional dependency on the position makes the values and the keys more expressive. The constraint required has been determined in [52], [48]. Considering unique multiplicities for clarity, if  $W_V^{kl}$  denotes the part of the matrix  $W_V$  multiplying the type- $l$  part of the vector  $\mathbf{f}$  to transform it to a type- $k$  vector, then the constraint has the form  $W_V^{kl}(R_r(\vec{x}_j - \vec{x}_i)) \mathbf{D}_l(r) = \mathbf{D}_k(r) W_V^{kl}(\vec{x}_j - \vec{x}_i)$ , for all  $r \in \text{SO}(3)$ . The same equation holds for the keys. The solution of this equation decomposes the matrix into a learnable part  $\phi_J$  depending only on the radius of the positions (which we parametrize by a lightweight MLP with

parameters  $\theta$ ), and a fixed part  $C_J$  depending on the angle as follows:

$$W_V^{kl}(\vec{x}_j - \vec{x}_i) = \sum_{J=|l-k|}^{l+k} \phi_J^{kl}(\|\vec{x}_j - \vec{x}_i\|; \theta) C_J^{kl} \left( \frac{\vec{x}_j - \vec{x}_i}{\|\vec{x}_j - \vec{x}_i\|} \right)$$

where  $C_J(\hat{x}) = \sum_{m=-J}^J Y_{Jm}(\hat{x}) Q_{Jm}^{kl}$ , with  $\hat{x} = \vec{x}/\|\vec{x}\|$ . Here  $Q_{Jm}^{kl} \in \mathbb{R}^{(2k+1) \times (2l+1)}$  are the Clebsch-Gordan matrices,  $Y_J : S^2 \rightarrow \mathbb{R}^{(2J+1)}$ , is the  $J^{\text{th}}$  real-valued spherical harmonic, and  $Y_{Jm}(\hat{x}) = [Y_J(\hat{x})]_m$  is its  $m$ -th coordinate.

Turning back to the non-linear attention module as a whole, [20] proposed to ensure that the output field is of  $\rho_{\text{out}}$ -type by obtaining from the value that already transforms the representation into such a field, and making the attention kernel  $\alpha(\cdot, \cdot)$  a type-0 (scalar) field, as a function of the positions. As we discussed, all finite-dimensional representations of  $\text{SO}(3)$  are equivalent to unitary ones, and so they preserve the standard inner product. Thus, if the query and key have the *same irreducible types*, then with  $W_Q^{ll}, W_K^{ll}$  denoting the blocks transforming a type- $l$  irreducible to a type- $l'$  one,

$$\begin{aligned} \langle W_Q^{ll} \mathbf{D}_l(r) \mathbf{f}_l, W_K^{ll}(\vec{x}_j - \vec{x}_i) \mathbf{D}_l(r) \mathbf{f}_l \rangle &= \langle \mathbf{D}_l(r) W_Q^{ll} \mathbf{f}_l, \mathbf{D}_l(r) W_K(R_r^{-1}(\vec{x}_j - \vec{x}_i)) \mathbf{f}_l \rangle \\ &= \langle W_Q^{ll} \mathbf{f}_l, W_K^{ll}(R_r^{-1}(\vec{x}_j - \vec{x}_i)) \mathbf{f}_l \rangle \end{aligned}$$

and for  $l \neq l'$ ,  $W_Q^{ll} = 0$  due to Schur's Lemma, and hence

$$\langle W_Q^{ll'} \mathbf{D}_l(r) \mathbf{f}_l, W_K^{ll'}(\vec{x}_j - \vec{x}_i) \mathbf{D}_l(r) \mathbf{f}_l \rangle = 0.$$

Thus the key, just as the query, can also have only the irreducible types that appear in the input.

In contrast to  $\mathcal{F}$ , the second network  $\mathcal{T}$  uses cross-attention modules. Its keys and values receive as input the local features  $\mathbf{f}_P = \{\mathbf{f}_{P_i}, i \in [N]\}$  output from the first network  $\mathcal{F}$ , i.e., the learned type-1 point cloud field. However, the queries now are of a different nature. We can assign a query token to any point  $\vec{q}$  in space. The query features  $\mathbf{f}_q$  are constructed again as type-1 vectors, as discussed in Section 3.2. The functional dependency  $Q(\vec{q}, \mathbf{f}_q) = W'_Q \mathbf{f}_q$  is similar to the one before, but for the same point cloud we can query an effectively infinite number of  $\vec{q} \in \mathbb{R}^3$ . After a composition of cross-attention layers, the output of the second network is the occupancy value at the point  $\vec{q}$ , where  $\mathcal{T}(\mathbf{f}_P, X, \mathbf{f}_q, \vec{q}) \in [0, 1]$ . The key, query and value matrices of  $\mathcal{T}$  satisfy the same constraints as the corresponding ones of  $\mathcal{F}$  to ensure equivariance.

If we denote with  $S_1$  the map that takes the input points  $X$  to produce the input features  $\mathbf{f}$  and  $S_2$  the map that takes  $\vec{q}$  to  $\mathbf{f}_{\vec{q}}$ , then we can prove that our whole pipeline is  $\text{SE}(3)$ -equivariant. Formally,

**Proposition 1.** *The map*

$$(X, \vec{q}) \rightarrow \mathcal{T}(\mathcal{F}[S_1(X), X], X, S_2(X, \vec{q}), \vec{q})$$

*is  $(\text{SE}(3), \mathcal{L}, \mathcal{L}')$ -equivariant, where  $\mathcal{L}$  acts on  $X$  according to (2) and on  $\vec{q}$  according to the standard representation. Moreover,  $\mathcal{L}'_{(t,r)} = I$ , for all  $(t, r) \in \text{SE}(3)$ .*

We provide a detailed proof in the Appendix. In addition to SE(3)-equivariance, the attention modules lead to a permutation equivariant architecture that can handle a variable number of points in the input. The network is trained with a standard binary cross-entropy loss, similarly to Occupancy Networks. We discuss experimental details in the next section.

For additional expressivity, *multi-headed* attention was proposed by [50]. Here an initial linear transformation projects the tokens in queries, keys and values to multiple feature vectors, followed by independent attention modules  $A(\cdot)$  applied in parallel. The concatenated result is linearly transformed to produce the output. We perform multi-headed attention by splitting the channels, i.e., the multiplicities of the irreducible representations; or, irreducibles. We also use skip connections and equivariant layer normalization as in [48], but defer these details to the Appendix. An overview of the method is discussed in Fig. 2.

It has been observed in [20] that equivariant networks constructed by interleaving SO(3)-equivariant linear layers with non-linearities on the norm [48] eliminate angular degrees of freedom while learning. The recent works [15,41] propose novel non-linearities to bypass this issue. On the other hand, attention modules are inherently non-linear, and the attention kernels are adaptive to the input, which help keep some angular degrees of freedom.

The local attention neighborhoods indicate that information flows only along each connected component of the point cloud-query graph. Moreover, our learned features give a local description of the point cloud. Thus, features are attached to points, in contrast to standard encoder-decoder architectures that create a global shape signature. This and the independence of our reconstruction of the position and orientation of an object implies that we can reconstruct scenes with an unknown number of objects, by training only on single objects. We perform this experiment in the next section.

**Comparison with Vector Neurons (VNN).** Compared to the VNN [15], our method exhibits the following key advantages:

- Our method extracts local features, which allows to reconstruct scenes with multiple objects, by composing features learned from single objects. On the other hand, the reconstruction of Vector Neurons is based on the Occupancy Network architecture, which uses a single global feature to model the reconstructed object.
- The SE(3)-equivariance of our model allows it to process inputs independent of their position in space. In contrast, the SO(3)-equivariant Vector Neurons model assumes that the objects are centered. This is particularly useful in scene reconstruction.

These two advantages—local shape modeling and SE(3)-equivariance—are the keys allowing our method to train on single objects and reconstruct scenes. In Section 4, we provide experiments comparing our method with Occupancy Networks and Vector Neurons, which perform global shape modeling, and with Convolutional Occupancy Networks, which perform local shape modeling but are only translation equivariant.

## 4 Experiments

We perform experiments on surface reconstruction from sparse and noisy input point clouds. We show the importance of SE(3)-equivariance by evaluating objects in various poses and positions in space. Additionally, we show the ability of our method to reconstruct novel scenes, even when *trained only on single objects*.

For the first network  $\mathcal{F}$ , we use ten multi-headed SE(3) attention layers, and for the second network  $\mathcal{T}$  we use another two multi-headed SE(3) attention layers. For each point  $\vec{x}_i$  of the point cloud, we define the neighborhood  $\mathcal{N}(\vec{x}_i)$  as its  $k$  nearest neighbors, where  $k$  is chosen to be 5% of the size of the point cloud ( $k=15$ ). During training, our method converges in around 200,000 iterations. This is faster than the methods we compare with, which require at least 300,000 iterations to converge. During inference, we approximate the object’s surface via the Marching Cubes algorithm [32].

### 4.1 Single Object Reconstruction from a Sparse point cloud

In our first experiment, we train and evaluate our model on sparse point clouds sampled from single objects in ShapeNet [7]. For each input shape, we uniformly sample 300 points from the ground truth mesh. Additionally each point is perturbed with normal noise with zero mean and a standard deviation of 0.005.

First we train and evaluate on the original objects from ShapeNet, where both the training and test data points are aligned to their canonical position (the  $I/I$  case). Additionally, we are interested in evaluating the performance of our method on data points with arbitrary poses. To achieve that, we follow [15] and evaluate on test data points that are transformed by random SO(3) rotations. We evaluate models that were trained on aligned training data (the  $I/SO(3)$  case), and models that were trained on data points augmented by SO(3) rotations (the  $SO(3)/SO(3)$  case). We compare with the Occupancy Network (OccNet) [35]—a non-equivariant network; with the Convolutional Occupancy Network (ConvOnet) [40]—a translation equivariant network that extracts local features; and with Vector Neurons (VNN) [15]—an SO(3) equivariant network.

In Table 1, we present the F-Score [47], the Chamfer-L1 distance [19] and the Intersection over Union (IoU) of the reconstruction, for models trained on the aligned and SO(3)-augmented datasets. We refer to section 6.2 of the Appendix material for a more detailed description of the evaluation metrics. Our method achieves consistent performance regardless of the rotation of the training or testing data points. This observation supports the results in section 3.3 showing that our method is equivariant. When both the training and test data are aligned, our method outperforms the SO(3)-equivariant VNN. Also, if the testing data are transformed by random SO(3) rotations, our method consistently outperforms the Occupancy Network, the Convolutional Occupancy Network and the VNN, regardless of whether it is trained on rotated or aligned training data.

In Figure 4, we show a qualitative comparison of the methods. Given the same input object in different poses, both our method and VNN outputs the same reconstruction, up to the corresponding rotation. However, our method captures

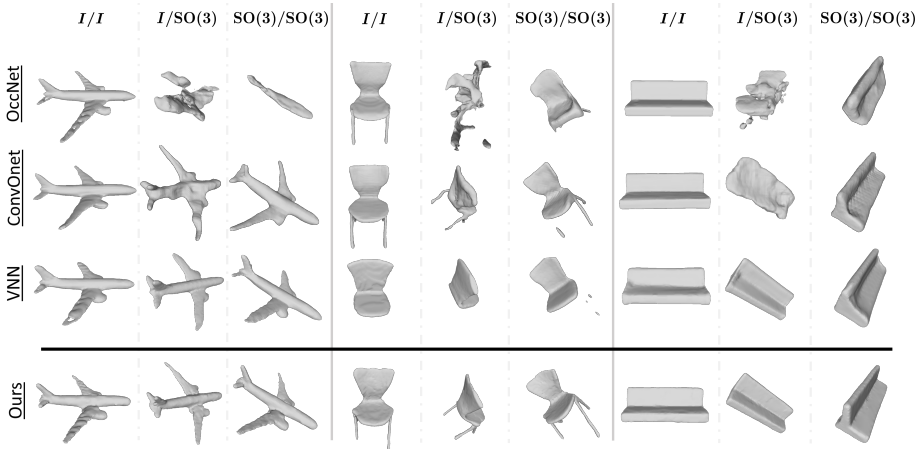


Fig. 4: Qualitative results using three methods for single object surface reconstruction trained and evaluated in three modes:  $I/I$  corresponds to models trained and tested on aligned shapes,  $I/SO(3)$  corresponds to models trained on aligned shapes and evaluated on rotated shapes,  $SO(3)/SO(3)$  corresponds to models trained and evaluated on rotated shapes.

more details in the objects than VNN. For example, the VNN consistently misses the legs of the chair in all poses, and slightly deforms the end of the sofa. Finally, in the  $SO(3)/SO(3)$  case, both the Occupancy Network and the Convolutional Occupancy Network achieve better results compared to the  $I/SO(3)$  case, but not on par with the  $I/I$  case. This shows that data augmentation is not enough to perform well on a rotated test set.

Table 1: Chamfer-L1 distance, F-Score and IoU achieved by OccNet, ConvOnet (grid  $32^3$ ), VNN, and our method on the experiment of single object reconstruction from sparse point clouds (300 points) sampled from ShapeNet.

	CHAMFER-L1 ↓			F-SCORE ( $\tau = 1\%$ ) ↑			F-SCORE ( $\tau = 2\%$ ) ↑			IoU ↑		
	$I/I$	$I/SO(3)$	$SO(3)/SO(3)$	$I/I$	$I/SO(3)$	$SO(3)/SO(3)$	$I/I$	$I/SO(3)$	$SO(3)/SO(3)$	$I/I$	$I/SO(3)$	$SO(3)/SO(3)$
OccNET	0.1	0.4	0.2	66.4%	21.4%	39.3%	89.7%	40.4%	65.6%	<b>77.8</b>	30.9%	58.2%
CONVONET	<b>0.093</b>	0.16	0.12	<b>71.7%</b>	43.9%	58.9%	<b>92.0%</b>	73.8%	85.6%	77.2	57.8%	71.2%
VNN	0.14	0.14	0.15	56.5%	56.5%	56.8%	81.2%	81.2	79.6%	69.3%	69.3%	68.8%
Ours	0.095	<b>0.095</b>	<b>0.098</b>	69.2%	<b>69.2%</b>	<b>69.2%</b>	90.9%	<b>90.9%</b>	<b>90.4%</b>	77.4%	<b>77.4%</b>	<b>77.3%</b>

## 4.2 Scene Reconstruction with Single Object Training

In this section, we evaluate the ability of our model to reconstruct novel scenes with many different objects, while *trained only on single objects*. We are interested in scenes where the objects are rotated and translated. Due to  $SE(3)$ -

equivariance, performance is consistent and independent to the pose and the position of the object. Additionally, our method performs computations in local neighborhoods that usually contain points from a single object. These two factors allow us to reconstruct scenes that contain objects in arbitrary poses and positions, without the need to train on similar scenes, or to segment into separate objects and reconstruct each independently.

**Seismic Dataset.** We construct a dataset of synthetic rooms with objects in arbitrary locations and poses. This is similar to the dataset constructed in [40], but we also perform random  $SO(3)$  rotations on each object. We call this dataset the *Seismic dataset*.

Each room contains objects from ShapeNet with random locations and orientations. Because we aim to evaluate models trained on single objects—and not whole scenes—we do not include walls, floor and ceiling in the rooms, since the models have not encountered such structures during training.

**Evaluation on Synthetic Rooms.** For the evaluation on the Seismic dataset, we want to have a uniform input from all objects in the scene. We achieve this by uniformly sampling 300 points from each object inside a scene. Methods that are trained only on single objects, and use a single feature vector to represent and reconstruct an object, fail completely in the setting of a scene, achieving IoU values of less than 10%. An example of such failure for Occupancy Networks and VNN is shown in Figure 5. On the contrary, due to the locality of our features, our model reconstructs each object in the scene independently. This, combined with the  $SE(3)$ -equivariance that guarantees a consistent performance regardless of the number, position and pose of the objects, allows our method to successfully reconstruct unseen scenes. We achieve an *IoU of 77.8%* on the same test set where the Occupancy Network and VNN fail with an IoU of *less than 10%*. The importance of  $SE(3)$ -equivariance is shown when we compare with ConvOnet which, similar to our method, uses local features, but is only translation equivariant. Even a ConvOnet trained on single objects augmented with random rotations achieves an *IoU of only 37%* on the Seismic dataset. Figure 6 shows more examples of reconstructions of our method on the Seismic dataset.

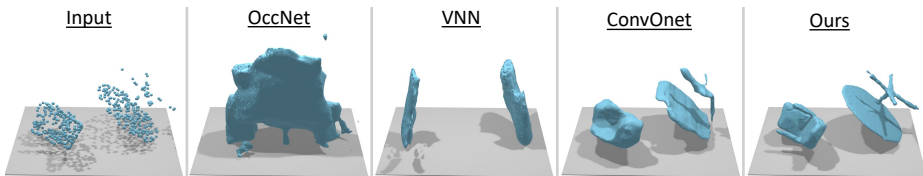


Fig. 5: Scene reconstructions using models trained on single objects.

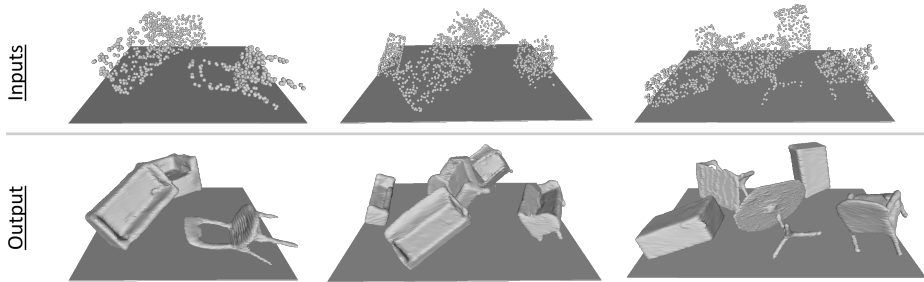


Fig. 6: Examples of scene reconstructions using our method, trained only on aligned single objects.

## 5 Conclusion

We proposed the first  $SE(3)$ -equivariant coordinate-based network for shape reconstruction. Our method is a fully attention-based pipeline consisting of two networks. The first, taking as input a sparse noisy point cloud, produces an equivariant local descriptor. The second takes as input this local descriptor and an arbitrary query point, and outputs the occupancy value of the query. Our equivariant construction ensures that the predicted occupancy function transforms as a scalar field. Thus, a simultaneous roto-translation of the point cloud and the query results in the same occupancy value. We evaluate our method against state of the art  $SO(3)$ -equivariant networks and non-equivariant methods trained with augmentations, and compare favorably in the single shape reconstruction category. Our coordinate-independent reconstruction and our local shape modelling procedure create an ideal setting for scene reconstruction tasks without ever training on scenes. While other methods fail completely, we perform as well as in the single object category.

## 6 Appendix

### 6.1 Matterport3D

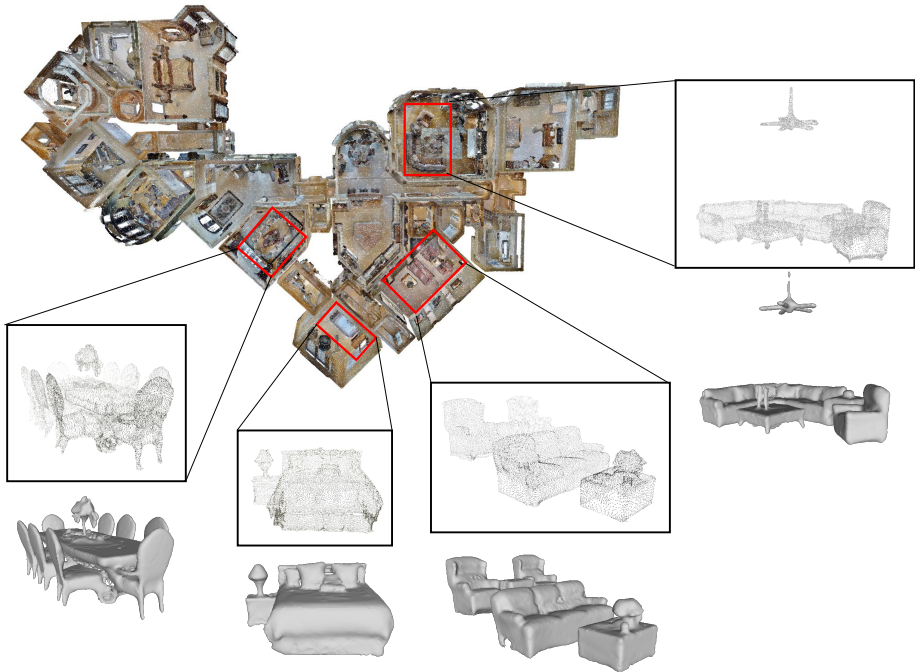


Fig. 7: Top part: Scene layout from Matterport3D [6] (with texture for visualization purposes only). Bottom part: Point cloud crops from the scene, and corresponding reconstructions from our method. Our model, produces remarkable **scene** reconstructions while being trained only on single, aligned **objects**, not from Matterport3D but from ShapeNet. Our *local shape modelling* design choice is particularly important, so that the model can adapt to the distribution shift between ShapeNet and Matterport3D that becomes as extreme as reconstructing completely unseen classes (see ceiling fan and candle sticks). Moreover, it results in a model that is agnostic to the number of objects in the scene, and that is able to handle variable sizes for reconstruction. Additionally,  $SE(3)$ -equivariance provides an advantage when reconstructing scenes with multiple objects, by guaranteeing a coordinate-consistent reconstruction. With this, reconstruction of arbitrarily placed objects with arbitrary orientations is feasible, even if we only train on single shapes of fixed orientations. The advantage of rotation equivariance is manifested even in scenes with “upward” oriented objects (see the dining room, where the chairs are roto-translated versions of each other).



In Section 4.2, we showed that our method reconstructs compositions of objects, even if it is trained on unique aligned objects. Here, we provide some examples of this behavior on real scenes from the Matterport3D dataset [6]. In Figure 7, we show reconstructions of input point cloud crops taken from a scan of a house contained in Matterport3D. The number of points contained in each crop varies from 6000 to 13000 points. Although during training our method has only seen aligned single objects from ShapeNet represented as point clouds of 300 points, it successfully reconstructs complicated realistic scenes containing multiple objects in arbitrary positions and poses, even from unseen classes (see the ceiling fan and the candle sticks).

## 6.2 Evaluation Metrics

In table 1, we presented the F-Score, Chamfer-L1 distance and Intersection over Union (IoU) of the reconstruction achieved by various models. For the F-Score and Chamfer-L1 distance, we compute the reconstructed mesh using the Marching Cubes algorithm. Then, we uniformly sample 100,000 points from the reconstructed mesh, and compare them with the “ground truth” points sampled similarly from the “ground truth” mesh. The standard deviation of the results for both metrics due to the randomness introduced by the sampling of the 100,000 points is smaller than  $10^{-5}$ . As defined in [47], the F-Score here is the harmonic mean between the precision and the recall of the reconstruction, where precision is the percentage of reconstructed points that lie within a certain distance  $\tau$  of the ground truth points, and recall is the percentage of ground truth points that lie within a distance  $\tau$  of the reconstructed points. We compute the F-Score with  $\tau$  equal to 1% of the side length of the reconstructed volume and with  $\tau$  equal to 2% of the side length of the reconstructed volume. For the IoU metric, we uniformly sample 100,000 points from the whole space, and compare the predicted occupancy to the ground truth occupancy. The IoU is then computed by taking the ratio between the points that are occupied according to both the predicted and the ground truth occupancy and the points that are occupied according to either the predicted or the ground truth occupancy.

## 6.3 Training and Testing Details

We train our model on the ShapeNet [7] subset constructed in [11]. We use the Adam [29] optimizer with learning that starts at  $2 \cdot 10^{-4}$  and linearly decreases to reach the value of  $10^{-5}$ . We train for 200,000 iterations using a batch size of 64. During training, we take as input a point cloud consisting of 300 points and as ground truth the occupancy value of 2048 points that are sampled uniformly inside a box that bounds the object. As a training loss, we use the binary cross-entropy loss between the predicted and the ground truth occupancy of the 2048 randomly sampled points.

During inference, recalling that the output of our model for one query point is in the range of  $[0, 1]$ , we classify a query point as occupied if the value of the learned occupancy function is above 0.2. After we query the occupancy of

points throughout the space, we reconstruct the object's mesh using the Marching Cubes algorithm [33].

## 6.4 Preliminaries

We recall some basic notions from group and representation theory, see e.g., [22]. A group  $(G, \cdot)$  is a set  $G$  together with a binary operator “ $\cdot$ ”:  $G \times G \rightarrow G$  that satisfies the following axioms:

- **Associativity:**  $g \cdot (h \cdot f) = (g \cdot h) \cdot f$  for all  $g, h, f \in G$
- **Identity:** there exists an element  $e \in G$  such that  $e \cdot g = g \cdot e = g$
- **Inverse:** for all  $g \in G$ , there exists  $g^{-1} \in G$  such that  $g^{-1} \cdot g = g \cdot g^{-1} = e$ .

Given  $G$ , we say that each group element  $g \in G$  acts on the space  $X$  via an **action**  $L_g : X \rightarrow X$  if  $L_g$  satisfy the following two properties:

- If  $e$  is the identity element of  $G$  then  $L_e[x] = x$  for all  $x \in G$ ;
- $L_g \circ L_h = L_{g \cdot h}$  for all  $g, h \in G$ .

If for any  $x, y \in X$  there exists  $g \in G$  such that  $L_g[x] = y$ , then we call  $X$  a homogeneous space for the group  $G$ .

When  $X = V$  is a vector space, we can define the group action using a **linear group representation**  $(V, \rho)$ , where  $\rho : G \rightarrow GL(V)$  is a map from group  $G$  to the general linear group  $GL(V)$ . This means that using the linear operator  $\rho(g)$  on  $V$ , we can define the group action  $L_g$  on the vector space  $V$  as  $L_g[x] = \rho(g)x$  for all  $x \in V, g \in G$ . Then  $(V, \rho)$  is a linear group representation if  $\rho$  is a group homomorphism, i.e.,  $\rho(g \cdot h) = \rho(g)\rho(h)$  for all  $g, h \in G$ , and  $\rho(e) = I_V$  is the identity operator over  $V$ . To simplify the notation, when the vector space  $V$  that the group acts on is easily inferred from the context, we will use  $\rho$  to denote the representation  $(V, \rho)$ .

Given a set of actions  $L_g : X \rightarrow X$  for  $g \in G$ , and a set of actions  $T_g : Y \rightarrow Y$  for  $g \in G$ , we say that a map  $f : X \rightarrow Y$  is  $(G, L, T)$ -equivariant if for every  $g \in G$ :

$$T_g[f(x)] = f(L_g[x]) \text{ for all } g \in G, x \in X.$$

If  $f$  is linear and equivariant (with respect to  $(G, L, T)$ ), then it is called an intertwiner (with respect to  $(G, L, T)$ ).

If there exists a subspace  $W \subset V$  such that for all  $g \in G$  and  $w \in W$ , we have that  $\rho(g)w \in W$ , then  $W$  is a  $G$ -invariant subspace of  $V$ , and  $(W, \rho)$  is a subrepresentation of  $(V, \rho)$ . All representations  $(V, \rho)$  have at least two subrepresentations:  $(0, \rho)$  and  $(V, \rho)$ . If a representation has no other subrepresentations, then it is called **irreducible**. Otherwise it is called reducible. A fundamental result is the following [22].

**Schur's Lemma** : Let  $(V, \rho_V)$ ,  $(W, \rho_W)$  be irreducible representations of  $G$  acting on  $V$  and  $W$ , respectively.

- If  $V$  and  $W$  are not isomorphic, then there are no nontrivial intertwiners between them.
- If  $V = W$  are finite-dimensional vector spaces over  $\mathbb{C}$ , and if  $\rho_V = \rho_W$ , then all intertwiners are scalar multiples of the identity.

Now we list a number of fundamental examples, see e.g., [22,25].

**The translation group  $(\mathbb{R}^3, +)$ :**  $\mathbb{R}^3$  equipped with the addition operator “+” is a group that is isomorphic to the group of translations in the 3D space.

**The special orthogonal group  $\text{SO}(3)$ :**  $\text{SO}(3)$  is the group of orthogonal matrices with determinant +1 equipped with multiplication; and is isomorphic to the group of all 3D rotations about the origin.  $\text{SO}(3)$  is a compact group and as a result of the Peter-Weyl theorem, its linear representations can be decomposed into a direct sum of finite-dimensional, unitary, irreducible representations. Specifically a linear representation of  $\text{SO}(3)$  decomposes as:

$$\rho(g) = Q^T \left[ \bigoplus_{J \geq 0} D_J(g) \right] Q \text{ for all } g \in G,$$

where  $Q$  is a change of basis matrix and for  $J = 0, 1, \dots$ ,  $D_J$  are  $(2J+1) \times (2J+1)$  matrices known as the Wigner D-matrices. The Wigner D-matrices are the irreducible representations of  $\text{SO}(3)$ . In the context of the features of a neural net, the representations (viewed as vectors) that transform according to  $D_J$  are called type- $J$  vectors.

**The special Euclidean group  $\text{SE}(3)$ :**  $\text{SE}(3)$  is the group of proper rigid transformations of 3D space, and is isomorphic to the semidirect product  $(\mathbb{R}^3, +) \rtimes \text{SO}(3)$ . An element of  $\text{SE}(3)$  can be represented as  $(t, r)$  where  $t$  is an element of the group of translations and  $r$  is an element of the group  $\text{SO}(3)$  of 3D rotations. For two elements  $(t_1, r_1), (t_2, r_2) \in \text{SE}(3)$ , the group law is defined as:

$$(t_1, r_1) \cdot (t_2, r_2) = (t_1 + r_1 t_2, r_1 r_2).$$

Since every point in  $\mathbb{R}^3$  can be transformed into any other point with a proper rigid transformation, we have that  $\mathbb{R}^3$  is a homogeneous space for  $\text{SE}(3)$ .

In addition to the action of  $\text{SE}(3)$  on vectors in  $\mathbb{R}^3$ , we can also define the action of  $\text{SE}(3)$  on functions  $f : \mathbb{R}^3 \rightarrow \mathbb{R}^M$ , for any given integer  $M > 0$ . This action is called the induced representation  $\pi = \text{Ind}_{\text{SO}(3)}^{\text{SE}(3)} \rho$  of  $\text{SE}(3)$ . It acts on  $f$  as follows:

$$[\pi((t, r))f](x) = \rho(r)f(r^{-1}(x - t)),$$

where  $(t, r) \in \text{SE}(3)$ ,  $x \in \mathbb{R}^3$  and  $\rho$  is a representation of  $\text{SO}(3)$ . Especially in the context of neural nets where functions are viewed as feature fields, a function that transforms according to  $\pi = \text{Ind}_{\text{SO}(3)}^{\text{SE}(3)}\rho$  is called a  $\rho$ -field, and if  $\rho$  corresponds to the  $l$ -th irreducible representation of  $\text{SO}(3)$ , it is also called a field of type- $l$ .

## 6.5 Architectural Details

The main module in our architecture is an  $\text{SE}(3)$ -equivariant attention block. Each block consists of a multi-head  $\text{SE}(3)$ -equivariant attention module followed by a skip connection and an equivariant layer normalization step.

**Multi-head  $\text{SE}(3)$ -equivariant Attention Module:** This module consists of multiple heads that implement either self-attention (input features for keys, values and queries are the same) or cross-attention (input features for keys and values are the same and different from the inputs for the queries). We will first describe the self-attention variant of the module and then describe the changes that are required for the cross-attention version.

The self-attention  $\text{SE}(3)$ -equivariant module takes as input a function  $f$  defined by  $f(\vec{x}) = \sum_{i=1}^N \mathbf{f}_i \delta(\vec{x} - \vec{x}_i)$ . Each one of the  $\mathbf{f}_i$  vectors can be decomposed into irreducible representations of  $\text{SO}(3)$  appearing with different multiplicities. This means that a single vector  $\mathbf{f}$  can be decomposed as  $\mathbf{f} = \bigoplus_{l>0} \bigoplus_{m_l \geq 0} \mathbf{f}_{l, m_l}$ , where  $\mathbf{f}_{l, m_l}$  corresponds to the  $m_l$ -th multiplicity of the irreducible component of type- $l$ . Since we perform self-attention, the keys, values and queries are computed using the same input function  $f$ . Specifically, for pairs of key and query points  $(\vec{x}_j, \vec{x}_i)$ , we compute the keys  $K(\mathbf{f}_j, \vec{x}_j, \vec{x}_i) = W_K(\vec{x}_j - \vec{x}_i)\mathbf{f}_j$ , the queries  $Q(\mathbf{f}_i, \vec{x}_i) = W_Q f_i$ , and the values  $V(\mathbf{f}_j, \vec{x}_j, \vec{x}_i) = W_V(\vec{x}_j - \vec{x}_i)\mathbf{f}_j$ . To ensure equivariance,  $W_K, W_Q, W_V$  must satisfy the conditions described in Section 3.3.

Suppose that for the computed key and query features, the  $l$ -th irreducible appears with multiplicity  $M_l$ , and for the computed value features the  $k$ -th irreducible appears with multiplicity  $N_k$ . For each irreducible, we split its multiplicities across the different heads of the attention block. Assuming that we have  $H$  heads in total, each head  $h$  receives keys  $K^{(h)}(\mathbf{f}_j, \vec{x}_j, \vec{x}_i)$  and queries  $Q^{(h)}(\mathbf{f}_i, \vec{x}_i)$  containing irreducibles with multiplicities  $M_l/H$  and receives values  $V^{(h)}(\mathbf{f}_k, \vec{x}_j, \vec{x}_i)$  containing irreducibles appearing with multiplicities  $N_k/H$ . After this split, the output of the self-attention for each head can be computed as:

$$\text{SA}^{(h)}[f, X](\vec{x}_i) = \sum_{\vec{x}_j \in \mathcal{N}(\vec{x}_i)} \alpha_X \left( Q^{(h)}(\mathbf{f}_i, \vec{x}_i), K^{(h)}(\mathbf{f}_j, \vec{x}_j, \vec{x}_i) \right) V^{(h)}(\mathbf{f}_j, \vec{x}_j, \vec{x}_i),$$

where

$$\alpha_X \left( Q(\mathbf{f}_i, \vec{x}_i), K(\mathbf{f}_j, \vec{x}_j, \vec{x}_i) \right) = \frac{\exp \left[ (Q(\mathbf{f}_i, \vec{x}_i))^T K(\mathbf{f}_j, \vec{x}_j, \vec{x}_i) \right]}{\sum_{\vec{x}_j \in \mathcal{N}(\vec{x}_i)} \exp \left[ (Q(\mathbf{f}_i, \vec{x}_i))^T K(\mathbf{f}_j, \vec{x}_j, \vec{x}_i) \right]}.$$

Similar to the keys, values and queries, the output can have irreducibles and multiplicities that differ from the input and decompose as:

$$\text{SA}^{(h)}[f, X] = \bigoplus_k \bigoplus_{n_k} \text{SA}^{(h)}[f, X]_{k, n_k},$$

where  $\text{SA}^{(h)}[f, X]_{k, n_k}$  is the  $n_k$ -th multiplicity of the  $k$ -th irreducible.

After the application of the self-attention layer, we concatenate the output of all the heads to create  $\text{SA}[f, X] = \bigoplus_h \text{SA}^{(h)}[f, X]$ . Then we pass the concatenated output through a linear SE(3)-equivariant layer to take  $\text{SA}^{\text{out}}[f, X] = W_P \text{SA}[f, X]$ . Since this linear layer needs also to be equivariant, it must follow the same constraints as the query matrix  $W_Q$ . By Schur’s lemma, it follows that  $W_P$  can only mix feature vectors that correspond to the same irreducibles.

For implementing cross-attention, we use the same process as with self-attention, with the only difference that the inputs for the queries are different from the inputs for the keys and the values. As a result, the output of the cross-attention for a single head  $h$  is computed as:

$$\text{CA}^{(h)}[f, X, \mathbf{f}_{\vec{q}}, \vec{q}] (\vec{q}) = \sum_{\vec{x}_j \in \mathcal{N}(\vec{q})} \alpha_X \left( Q^{(h)}(\mathbf{f}_{\vec{q}}, \vec{q}), K^{(h)}(\mathbf{f}_j, \vec{x}_j, \vec{q}) \right) V^{(h)}(\mathbf{f}_j, \vec{x}_j, \vec{q}).$$

**Skip connection:** The skip connection concatenates the output features of the multi-head SE(3)-equivariant module with the features of the input query. To respect the type of each feature, this concatenation must happen between features corresponding to the same irreducible.

Suppose that  $\mathbf{f}^{\text{out}}$  is the output of the multi-head attention, decomposing into irreducibles and their multiplicities as  $\mathbf{f}^{\text{out}} = \bigoplus_k \bigoplus_{n_k} \mathbf{f}_{k, n_k}^{\text{out}}$ . Similarly suppose that  $\mathbf{f}_{\vec{q}}$  is the input query, decomposing into irreducibles and their multiplicities as  $\mathbf{f}_{\vec{q}} = \bigoplus_l \bigoplus_{m_l} \mathbf{f}_{\vec{q}, (l, m_l)}$ . The application of the skip connection gives an output:

$$\mathbf{f}^{\text{skip}} = \bigoplus_k \left[ \left( \bigoplus_{n_k} \mathbf{f}_{k, n_k}^{\text{out}} \right) \oplus \left( \bigoplus_{m_k} \mathbf{f}_{\vec{q}, (k, m_k)} \right) \right].$$

**Equivariant Layer Norm:** Suppose that  $\mathbf{f}_{l, m}$  denotes the  $m$ -th type- $l$  irreducible of the input vector  $\mathbf{f}$ . As proposed in [20], for each vector  $\mathbf{f}_{l, m}$ , we apply layer normalization and a nonlinearity on the norm of  $\mathbf{f}_{l, m}$ , leaving its direction unchanged. Thus, the equivariant normalization layer can be written as:

$$\text{EqLayerNorm}(f)_{l, m} = \text{ReLU} \left( \text{LayerNorm} \left( \bigoplus_m \|\mathbf{f}_{l, m}\| \right) \right)_m \frac{\mathbf{f}_{l, m}}{\|\mathbf{f}_{l, m}\|},$$

where LayerNorm corresponds to the layer normalization that was proposed in [2].

We use the SE(3)-equivariant attention block to construct both the network  $\mathcal{F}$  that assigns to each point in the point cloud a type-1 feature, and the network

$\mathcal{T}$ , that outputs the occupancy value of a query point in space. The network  $\mathcal{F}$  consists of ten SE(3)-equivariant self-attention blocks, and  $\mathcal{T}$  consists of two SE(3)-equivariant cross-attention blocks. Figure 2 shows a diagram of this architecture.

In both networks, we use blocks with eight heads and intermediate representations that contain both type-0 and type-1 features. Additionally, for each type we set the multiplicity of the corresponding irreducible to 32. Finally, for the computation of the local neighborhood  $\mathcal{N}(\vec{x})$  around each point  $\vec{x}$ , we use the  $k$  nearest neighbors with  $k = 15$ .

Although it is possible for  $\mathcal{T}$  to output a single scalar that corresponds to the occupancy value at a queried point, we observe in the experiments an increase in performance when  $\mathcal{T}$  outputs 32 scalar values that we then pass through a simple MLP to get the final occupancy value.

## 6.6 Proof of Proposition 1

The proof has three main steps. To show that the map is  $(\text{SE}(3), \mathcal{L}_{\text{in}}, \mathcal{L}_{\text{out}})$ -equivariant, we first prove that the operator  $\mathcal{L}_{\text{in}}$  describes a group action on the input point cloud and query. Next, we show that the input features to the self- and cross- attention layers are type-1 fields. Lastly, we show that given an arbitrary  $\rho_{\text{in}}$ -field as input, each attention block produces a  $\rho_{\text{out}}$ -field. In other words, these blocks are equivariant to an induced representation. By induction, we find that the final output after composing any number of such blocks is also a  $\rho$ -field. Choosing it to be of type-0, we conclude that  $\mathcal{L}'_{\text{out}}$  is the trivial (identity) action.

**Step 1:** As we describe in the main text, we start from a point cloud, represented by an  $N \times 3$  matrix  $X = [\vec{x}_i^T]_{i=1, \dots, N}$ , where we concatenate the position vectors  $\vec{x}_i$  of the points row-wise. We also use the notation  $X = \oplus_{i=1}^N [\vec{x}_i]^T$ . Since the abstract group of proper rigid transformations is isomorphic to SE(3) and also to the semidirect product  $\mathbb{R}^3 \rtimes \text{SO}(3)$ , we overload the notation and write  $(t, r) \in \text{SE}(3)$  for the abstract group elements. We also write  $R_r \in \text{SO}(3)$  for the 3D rotation matrices and  $T_t \in \mathbb{R}^3$ , for the 3D translation vectors that correspond to the second isomorphism.

We will first show that (2), namely  $\mathcal{L}_{(t,r)}[X] = XR_r^T + \oplus_N T_t^T$ , for all  $(t, r) \in \text{SE}(3)$ , indeed describes a group action on  $X$ . Letting  $(e, e)$  be the identity element of SE(3), we can check that

$$\mathcal{L}_{(e,e)}[X] = XR_e^T + \oplus_N T_e^T = XI_3^T + \oplus_N 0_3^T = X.$$

For any  $(t_1, r_1), (t_2, r_2)$  from  $\text{SE}(3)$ , we can check that

$$\begin{aligned}
\mathcal{L}_{(t_2, r_2)}[\mathcal{L}_{(t_1, r_1)}[X]] &= (X R_{r_1}^T + \oplus_N T_{t_1}^T) R_{r_2}^T + \oplus_N T_{t_2}^T = \\
&= X R_{r_1}^T R_{r_2}^T + (\oplus_N T_{t_1}^T) R_{r_2}^T + \oplus_N T_{t_2}^T \\
&= X R_{r_1}^T R_{r_2}^T + \oplus_N (T_{t_1}^T R_{r_2}^T + T_{t_2}^T) \\
&= X (R_{r_2} R_{r_1})^T + \oplus_N (R_{r_2} T_{t_1} + T_{t_2})^T \\
&= X R_{r_2 r_1}^T + \oplus_N T_{r_2 t_1 + t_2}^T = \mathcal{L}_{r_2 t_1 + t_2, r_2 r_1}[X] \\
&= \mathcal{L}_{[(t_2, r_2) \cdot (t_1, r_1)]}[X].
\end{aligned}$$

Using the vector space isomorphism associating  $X \in \mathbb{R}^{N \times 3}$  with the unrolled vector  $\text{vec}(X) \in \mathbb{R}^{3N}$ , we can view this action as the direct sum of  $N$  standard representations.

The action  $\mathcal{L}_{\text{in}}$  applied to  $(X, \vec{q})$  produces  $\mathcal{L}_{\text{in}, (t, r)}[(X, \vec{q})] = (\mathcal{L}_{(t, r)}[X], R_r \vec{q} + T_t)$ . This is equivalent to the direct sum of  $N + 1$  standard representations, if we concatenate  $\vec{q}$  row-wise to  $X$ .

**Step 2:** For the  $i$ -th point at position  $\vec{x}_i$ , we construct a feature  $\mathbf{f}_i$  as input to the first self attention layer of  $\mathcal{F}$ . We select the feature  $\mathbf{f}_i$  as the relative position of the  $i$ -th point,  $\vec{x}_i$ , to the centroid of a neighborhood constructed from its  $k$  nearest neighbors in the point cloud in Euclidean norm, i.e.,

$$\mathbf{f}_i(X) = \vec{x}_i - \frac{1}{|\mathcal{N}_i^k(X)|} \sum_{j \in \mathcal{N}_i^k(X)} \vec{x}_j, \quad X = \oplus_{i=1}^N [\vec{x}_i]^T,$$

where

$$\mathcal{N}_i^k(X) = \{j \in [N] \mid \|\vec{x}_i - \vec{x}_j\|_2 \leq \|\vec{x}_i - \vec{x}_k^{(i)}\|_2\}$$

is the neighborhood of the  $i$ -th point in the point cloud. Also,  $(\vec{x}_j^{(i)})_{j \in [N]}$  is a sorting of the points in the point cloud in increasing Euclidean distance to the  $i$ -th point, i.e.,  $\|\vec{x}_i - \vec{x}_1^{(i)}\|_2 \leq \dots \leq \|\vec{x}_i - \vec{x}_N^{(i)}\|_2$ . In case of ties, we assign numbers randomly. Due to the use of “ $\leq$ ” (instead of the strict inequality symbol “ $<$ ”), in the definition of the neighborhoods, if there are ties for  $\vec{x}_k^{(i)}$ , we include all tied points in the neighborhood.

Now we study how the features  $\mathbf{f}_i$  transform when the points in the point cloud transform via  $\mathcal{L}_{(t, r)}$ , discussed in the first step. Since

$$\mathcal{L}_{(t, r)}[X] = \oplus_{i=1}^N (\mathcal{L}_{(t, r)}[X]_i) = \oplus_{i=1}^N [R_r \vec{x}_i + T_t]^T,$$

we find:

$$\begin{aligned}
\mathbf{f}_i(\mathcal{L}_{(t, r)}[X]) &= \mathcal{L}_{(t, r)}[X]_i - \frac{1}{|\mathcal{N}_i^k(\mathcal{L}_{(t, r)}[X])|} \sum_{j \in \mathcal{N}_i^k(\mathcal{L}_{(t, r)}[X])} \mathcal{L}_{(t, r)}[X]_j \\
&= (R_r \vec{x}_i + T_t) - \frac{1}{|\mathcal{N}_i^k(X)|} \sum_{j \in \mathcal{N}_i^k(X)} (R_r \vec{x}_j + T_t),
\end{aligned}$$

where we used the claim, proved below, that

$$\mathcal{N}_i^k(\mathcal{L}_{(t,r)}[X]) = \mathcal{N}_i^k(X). \quad (3)$$

Thus,  $\mathbf{f}_i(\mathcal{L}_{(t,r)}[X])$  further equals

$$R_r \left( \vec{x}_i - \frac{1}{|\mathcal{N}_i^k(X)|} \sum_{j \in \mathcal{N}_i^k(X)} \vec{x}_j \right) = R_r \mathbf{f}_i(X), \text{ for all } (t, r) \in \text{SE}(3).$$

We now prove (3). When all  $\vec{x}_i$  are mapped as  $\vec{x}_i \xrightarrow{\mathcal{L}_{(t,r)}} R_r \vec{x}_i + T_t$ , the Euclidean distance between any two points is preserved, i.e.,  $\|(R_r \vec{x}_i + T_t) - (R_r \vec{x}_j + T_t)\|_2 = \|\vec{x}_i - \vec{x}_j\|_2$ . Thus, if before the transformation  $\|\vec{x}_i - \vec{x}_k^{(i)}\|_2 = d_k$ , then after the transformation we also have  $\|\mathcal{L}[X]_i - \mathcal{L}[X]_k^{(i)}\|_2 = d_k$ . This is because all nearest neighbors preserve their distances, and thus sorting returns the same indices up to random tie breaking. Thus,

$$\begin{aligned} j \in \mathcal{N}_i^k(X) &\iff \|\vec{x}_i - \vec{x}_j\|_2 \leq d_k \\ &\iff \|(R_r \vec{x}_i + T_t) - (R_r \vec{x}_j + T_t)\|_2 \leq d_k \\ &\iff \|\mathcal{L}[X]_i - \mathcal{L}[X]_j\|_2 \leq d_k \\ &\iff \|\mathcal{L}[X]_i - \mathcal{L}[X]_j\|_2 \leq \|\mathcal{L}[X]_i - \mathcal{L}[X]_k^{(i)}\|_2 \\ &\iff j \in \mathcal{N}_i^k(\mathcal{L}[X]) \end{aligned}$$

The first and fourth equivalence hold because we include *all* tied neighbors in the neighborhood. Thus, the neighborhood is defined by the *distance*  $d_k$ , and not by the identity of the  $k$ -neighbors.

Thus  $\mathbf{f}_i$  transforms according to the standard representation of  $\text{SO}(3)$  when each point in the point cloud transforms according to the standard representation of  $\text{SE}(3)$ . If we view the features as a function on the point cloud extended to the homogeneous space  $\mathbb{R}^3 \cong \text{SE}(3)/\text{SO}(3)$ , i.e.,  $f(x) = \sum_{i=1}^N \mathbf{f}_i \delta(x - x_i)$ , then this function transforms according to the *induced representation* discussed in the main text as:

$$\mathcal{L}_{(t,r)}^{(ind)}[f](\vec{x}) = R_r f(R_r^{-1}(\vec{x} - T_r)) = \sum_{i=1}^N (R_r \mathbf{f}_i) \delta((R_r^{-1}(\vec{x} - T_t) - \vec{x}_i)).$$

Recall that functions transforming according to the above law are called type-1 fields. We will keep the name, but avoid the Dirac notation, keeping the matrix notation instead. By concatenating the features row-wise, we find the map, described in the main text as  $S_1$ , i.e.,  $S_1(X) = \oplus_{i=1}^N \mathbf{f}_i^T$ .

Now we turn to the second network  $\mathcal{T}$ . For each point  $\vec{q} \in \mathbb{R}^3$  whose occupancy value we wish to find, we first construct a feature  $\mathbf{f}_{\vec{q}}$  similarly to before, and then use the pair  $(\vec{q}, \mathbf{f}_{\vec{q}})$  as the query to the first cross-attention layer of  $\mathcal{T}$ . We will show that, when the query  $\vec{q}$  transforms according to the standard



representation of  $\text{SE}(3)$ , this input feature  $\mathbf{f}_{\vec{q}}$  also transforms according to the standard representation of  $\text{SO}(3)$ .

We again construct the feature  $\mathbf{f}_{\vec{q}}$  as the relative position between  $\vec{q}$  and the centroid of its neighborhood  $\mathcal{N}_X^Q(\vec{q})$ . We consider  $\mathcal{N}_X^Q(\vec{q})$  to be the same as the neighborhood of its closest—in Euclidean distance—point in the point cloud, and write (if the closest point is defined uniquely)

$$\mathcal{N}_X^Q(\vec{q}) := \mathcal{N}_{\arg \min_{i \in [N]} (\|\vec{q} - \vec{x}_i\|_2)}^k(X).$$

We discuss at the end of this step the case where the nearest neighbors are tied. At the moment, let the unique closest point be  $c = \arg \min_{i \in [N]} (\|\vec{q} - \vec{x}_i\|_2)$ . Then, the query feature becomes:

$$\begin{aligned} \mathbf{f}_{\vec{q}}(X, \vec{q}) &= \vec{q} - \frac{1}{|\mathcal{N}_X^Q(\vec{q})|} \sum_{j \in \mathcal{N}_X^Q(\vec{q})} \vec{x}_j \\ &= \vec{q} - \frac{1}{|\mathcal{N}_c^k(X)|} \sum_{j \in \mathcal{N}_c^k(X)} \vec{x}_j, \quad X = \oplus_{i=1}^N [\vec{x}_i]^T. \end{aligned} \quad (4)$$

The proof that

$$\mathbf{f}_{(R_r \vec{q} + T_t)}(\mathcal{L}_{(t,r)}[X], R_r \vec{q} + T_t) = R_r \mathbf{f}_{\vec{q}}$$

holds due to the same arguments as the proof for  $\mathbf{f}_i$  above. Viewed again as a function defined on  $\mathbb{R}^3$ , the map  $f_Q$  with  $f_Q(\vec{q}) = \mathbf{f}_{\vec{q}}$  constitutes a type-1 field. The transformation law of this field is depicted in Fig. 3, described in the main text as  $S_2$ .

**Remark:** When there are ties, i.e., the set  $\arg \min_{i \in [N]} (\|\vec{q} - \vec{x}_i\|_2)$  contains more than one point, we form all neighborhoods

$$\mathcal{N}_X^Q(\vec{q}) = \{\mathcal{N}_c^k(X) \mid c \in \arg \min_{i \in [N]} \|\vec{q} - \vec{x}_i\|_2\}.$$

Then, we consider a query token for each pair  $(\vec{q}^c, \mathbf{f}_{\vec{q}}^c)$ , where  $\vec{q}^c = \vec{q}$  and  $\mathbf{f}_{\vec{q}}^c$  are constructed as in (4), using the neighborhood  $\mathcal{N}_c^k(X) \in \mathcal{N}_X^Q(\vec{q})$ .

If  $\mathbf{f}_{\vec{q}}^c$  transforms as a type-1 field, then, after the roto-translation of the point cloud and the query, we could identify the same  $c$  as a closest neighbor. However, since those points are equivalent as nearest neighbors, we will process the whole set of fields independently, producing a set of fields in the output. A different order of selection of nearest neighbors after the roto-translation corresponds to a permutation of the set of the output fields. Since attention modules are permutation equivariant, this permutation propagates to the output.

We only need to discuss how to combine these outputs on the tokens  $\vec{q}^c$  that correspond to the same position  $\vec{q}$  in the occupancy field. Since the output is a scalar field (as we prove next), we can take the maximum across the same channels to construct a new scalar field that is also invariant to any permutation. The idea is that taking the maximum corresponds to an ‘‘OR’’ operation, since both the usual non-linearities (such as the sigmoid) and the thresholding

operations that follow are increasing functions of their inputs. Thus, when the network predicts that the position of the query is “occupied”, even based on one neighborhood, the position is likely to be considered occupied.

**Step 3:** In this step we will prove that, given an input field of a certain type, each self- and cross- attention layer produces an output field of a certain—usually different—type. For simplicity we prove the result for one attention head. It will be clear from the proof that a concatenation of the heads and a subsequent linear transformation mixing channels that correspond to the same irreducible preserves equivariance.

We start with the self-attention layers in  $\mathcal{F}$ . We have already proven that the input to the first layer transforms as a type-1 field. For an arbitrary layer, consider a  $\rho_{\text{in}}$ -field of the form  $f^{\text{in}}(\vec{x}) = \sum_{i=1}^N \mathbf{f}_i^{\text{in}} \delta(\vec{x} - \vec{x}_i)$  in the input. If we concatenate the features row-wise as:  $\mathbf{F}(X = \oplus_{i=1}^N [\vec{x}_i]^T) = \oplus_{i=1}^N \mathbf{f}_i^T$  then  $f^{\text{in}}$  is a  $\rho_{\text{in}}$ -field if and only if:

$$\mathbf{F}(\mathcal{L}_{(t,r)}[X]) = \mathbf{F}(X)\rho_{\text{in}}^T(r). \quad (5)$$

By the Peter-Weyl theorem, this field decomposes into unitary, irreducible representations of  $\text{SO}(3)$ , possibly with multiplicities. Thus,

$$\rho_{\text{in}}(r) = Q_{\text{in}}^T \left( \bigoplus_l \bigoplus_{m_l} \mathbf{D}_l(r) \right) Q_{\text{in}}, \quad r \in \text{SO}(3),$$

where in our case  $Q_{\text{in}} = I$ ,  $\bigoplus$  for matrices denotes a concatenation along the diagonal and  $l$  indexes the irreducible types and  $m_l$  indexes the multiplicity of the  $l$ -th irreducible. Then, for each  $\vec{x}$  in the point cloud (where we suppress the index  $i$  for clarity), we have  $\mathbf{f}^{\text{in}} = \bigoplus_l \bigoplus_{m_l} \mathbf{f}_{l,m_l}^{\text{in}}$ . We also consider an output field transforming according to  $\rho_{\text{out}} = Q_{\text{out}}^T (\bigoplus_k \bigoplus_{n_k} \mathbf{D}_k(r)) Q_{\text{out}} - Q_{\text{out}} = I$  in our case—that decomposes as  $\mathbf{f}^{\text{out}} = \bigoplus_k \bigoplus_{n_k} \mathbf{f}_{k,n_k}^{\text{out}}$ . The goal is to show that our attention layers can transform the  $\rho_{\text{in}}$ -field to the  $\rho_{\text{out}}$ -field.

The self-attention layer from Section 3.3 outputs at the  $i$ -th output token:

$$\text{SA}[\mathbf{F}(X), X]_i = \sum_{j \in \mathcal{N}_i^k(X)} \alpha_X [Q(\mathbf{f}_i, \vec{x}_i), K(\mathbf{f}_j, \vec{x}_j, \vec{x}_i)] \underbrace{W_V(\vec{x}_j - \vec{x}_i) \mathbf{f}_j}_{V(\mathbf{f}_j, \vec{x}_j, \vec{x}_i)},$$

where the attention kernel  $\alpha_X$  takes the form:

$$\begin{aligned} \alpha_X [Q(\mathbf{f}_i, \vec{x}_i), K(\mathbf{f}_j, \vec{x}_j, \vec{x}_i)] &= \frac{\exp [(Q(\mathbf{f}_i, \vec{x}_i))^T K(\mathbf{f}_j, \vec{x}_j, \vec{x}_i)]}{\sum_{j \in \mathcal{N}_i^k(X)} \exp [(Q(\mathbf{f}_i, \vec{x}_i))^T K(\mathbf{f}_j, \vec{x}_j, \vec{x}_i)]} \\ &= \frac{\exp [(W_Q \mathbf{f}_i)^T (W_K(\vec{x}_j - \vec{x}_i) \mathbf{f}_j)]}{\sum_{j \in \mathcal{N}_i^k(X)} \exp [(W_Q \mathbf{f}_i)^T (W_K(\vec{x}_j - \vec{x}_i) \mathbf{f}_j)]}, \quad i \in [N]. \end{aligned}$$

The goal is to prove that:

$$\text{SA}[\mathbf{F}(\mathcal{L}_{(t,r)}[X]), \mathcal{L}_{(t,r)}[X]]_i = \rho_{\text{out}}(r) \text{SA}[\mathbf{F}[X], X]_i, \quad \text{for all } (t, r) \in \text{SE}(3).$$

Consider now the constraints obeyed by the matrix  $W_Q$  and the matrix functions  $W_K, W_V$  from Section 3.3. Recall that each of these matrices are of dimension  $\sum_k \sum_{n_k} (2k+1) \times \sum_l \sum_{m_l} (2l+1)$ .

1. For  $W_Q$ , we have

$$\rho_{\text{out}}(r)W_Q = W_Q\rho_{\text{in}}(r), \text{ for all } r \in \text{SO}(3). \quad (6)$$

By Schur's Lemma, for each block  $[W_Q]_{l,m_l}^{k,n_k}$  that multiplies  $\mathbf{f}_{l,m_l}^{\text{in}}$  to create  $\mathbf{f}_{k,n_k}^{\text{out}}$  (after adding all contributions), we have, for some constants  $c_{l,m_l}^{k,n_k}$ :

$$[W_Q]_{l,m_l}^{k,n_k} = \begin{cases} 0 & \text{if } l \neq k \\ c_{l,m_l}^{k,n_k} I_{2l+1} & \text{if } l = k. \end{cases}$$

Thus the query cannot transform an irreducible type to another irreducible type, but only mix channels that correspond to the same irreducible. However, (6) clearly holds.

2. For  $W_V$ , the constraint is that for all  $r \in \text{SO}(3)$ , the following set of equivalent statements holds:

$$\begin{aligned} W_V(R_r(\vec{x}_j - \vec{x}_i))\rho_{\text{in}}(r) &= \rho_{\text{out}}(r)W_V(\vec{x}_j - \vec{x}_i) \iff \\ W_V(R_r(\vec{x}_j - \vec{x}_i))\left[\bigoplus_{l,m_l} \mathbf{D}_l(r)\right] &= \left[\bigoplus_{k,n_k} \mathbf{D}_k(r)\right]W_V(\vec{x}_j - \vec{x}_i) \iff \\ [W_V(R_r(\vec{x}_j - \vec{x}_i))]_{l,m_l}^{k,n_k} \mathbf{D}_l(r) &= \mathbf{D}_k(r)[W_V(\vec{x}_j - \vec{x}_i)]_{l,m_l}^{k,n_k}. \end{aligned}$$

The solution, as discussed in the main text and solved in [52,48] is:

$$[W_V(\vec{x}_j - \vec{x}_i)]_{l,m_l}^{k,n_k} = \sum_{J=|l-k|}^{l+k} \phi_{J,l,m_l}^{k,n_k}(\|\vec{x}_j - \vec{x}_i\|; \theta) C_{J,l,k} \left( \frac{\vec{x}_j - \vec{x}_i}{\|\vec{x}_j - \vec{x}_i\|} \right),$$

where  $C_{J,l,k}(\hat{x}) = \sum_{m=-J}^J Y_{Jm}(\hat{x}) Q_{Jm}^{kl}$ ,  $Q_{Jm}^{kl} \in \mathbb{R}^{(2k+1) \times (2l+1)}$  are the Clebsch-Gordan matrices,  $Y_J : S^2 \rightarrow \mathbb{R}^{(2J+1)}$ , is the  $J$ -th real spherical harmonic,  $Y_{Jm}(\hat{x}) = [Y_J(\hat{x})]_m$  is its  $m$ -th coordinate, and  $\hat{x} = \vec{x}/\|\vec{x}\|$ .

3. For  $W_K$ , we have the same equation as for  $W_V$  above:

$$W_K(R_r(\vec{x}_j - \vec{x}_i))\rho_{\text{in}}(r) = \rho_{\text{out}}(r)W_K(\vec{x}_j - \vec{x}_i),$$

but in addition we constrain the blocks between different irreducible types to be zero, i.e.,

$$[W_K(\vec{x}_j - \vec{x}_i)]_{l,m_l}^{k,n_k} = 0, \text{ if } k \neq l.$$

For the attention layer, we have for  $X = \bigoplus_{i=1}^N [\vec{x}_i]^T$  and for each output token  $i \in [N]$ :

$$\begin{aligned}
\text{SA}[\mathbf{F}(\mathcal{L}_{(t,r)}[X]), \mathcal{L}_{(t,r)}[X]]_i &= \text{SA}[\mathbf{F}(X)\rho_{\text{in}}^T(r), \mathcal{L}_{(t,r)}[X]]_i = & (7) \\
&= \sum_{j \in \mathcal{N}_i^k(\mathcal{L}_{(t,r)}[X])} \alpha_{\mathcal{L}_{(t,r)}[X]} [Q(\rho_{\text{in}}(r)\mathbf{f}_i, R_r\vec{x}_i + T_t), K(\rho_{\text{in}}(r)\mathbf{f}_j, R_r\vec{x}_j + T_t, R_r\vec{x}_i + T_t)] \cdot \\
&W_V((R_r\vec{x}_j + T_t) - (R_r\vec{x}_i + T_t))\rho_{\text{in}}(r)\mathbf{f}_j \\
&= \sum_{j \in \mathcal{N}_i^k(X)} \alpha_{\mathcal{L}_{(t,r)}[X]} [W_Q\rho_{\text{in}}(r)\mathbf{f}_i, W_K(R_r(\vec{x}_j - \vec{x}_i))\rho_{\text{in}}(r)\mathbf{f}_j] W_V(R_r(\vec{x}_j - \vec{x}_i))\rho_{\text{in}}(r)\mathbf{f}_j,
\end{aligned}$$

where in the first equation we used (5) for the transformation law of the field  $\mathbf{F}(X)$ , in the second we applied the transformation element-wise, and in the third, we used (3) for the invariant neighborhoods,  $\mathcal{N}_i^k(\mathcal{L}_{(t,r)}[X]) = \mathcal{N}_i^k(X)$ . Now using the constraints for the matrices we find for each term  $j \in \mathcal{N}_i^k(X)$  that the individual terms in the above sum equal:

$$\begin{aligned}
&\alpha_{\mathcal{L}_{(t,r)}[X]} [\rho_{\text{out}}(r)W_Q\mathbf{f}_i, \rho_{\text{out}}(r)W_K(\vec{x}_j - \vec{x}_i)\mathbf{f}_j] \rho_{\text{out}}(r)W_V(\vec{x}_j - \vec{x}_i)\mathbf{f}_j \\
&= \rho_{\text{out}}(r)\alpha_{\mathcal{L}_{(t,r)}[X]} [\rho_{\text{out}}(r)W_Q\mathbf{f}_i, \rho_{\text{out}}(r)W_K(\vec{x}_j - \vec{x}_i)\mathbf{f}_j] W_V(\vec{x}_j - \vec{x}_i)\mathbf{f}_j, \quad (8)
\end{aligned}$$

where in the second equation we used that the attention kernel gives a scalar output. Now, the attention kernel from the last equation transforms as

$$\begin{aligned}
&\alpha_{\mathcal{L}_{(t,r)}[X]} [\rho_{\text{out}}(r)W_Q\mathbf{f}_i, \rho_{\text{out}}(r)W_K(\vec{x}_j - \vec{x}_i)\mathbf{f}_j] = \\
&= \frac{\exp[(\rho_{\text{out}}(r)W_Q\mathbf{f}_i)^T(\rho_{\text{out}}(r)W_K(\vec{x}_j - \vec{x}_i)\mathbf{f}_j)]}{\sum_{j \in \mathcal{N}_i^k(\mathcal{L}_{(t,r)}[X])} \exp[(\rho_{\text{out}}(r)W_Q\mathbf{f}_i)^T(\rho_{\text{out}}(r)W_K(\vec{x}_j - \vec{x}_i)\mathbf{f}_j)]} = \\
&= \frac{\exp[(W_Q\mathbf{f}_i)^T(W_K(\vec{x}_j - \vec{x}_i)\mathbf{f}_j)]}{\sum_{j \in \mathcal{N}_i^k(X)} \exp[(W_Q\mathbf{f}_i)^T(W_K(\vec{x}_j - \vec{x}_i)\mathbf{f}_j)]} = \alpha_X [Q(\mathbf{f}_i, \vec{x}_i)K(\mathbf{f}_j, \vec{x}_j, \vec{x}_i)], \quad (9)
\end{aligned}$$

where we used again the properties of the invariant neighborhoods and that  $\rho_{\text{out}}$  is a unitary representation, i.e.,  $\rho_{\text{out}}(r)^T \rho_{\text{out}}(r) = I$  for all  $r \in \text{SO}(3)$ .

Using (8), (9), and (7), we find:

$$\begin{aligned}
&\text{SA}[\mathbf{F}(\mathcal{L}_{(t,r)}[X]), \mathcal{L}_{(t,r)}[X]]_i \\
&= \rho_{\text{out}}(r) \sum_{j \in \mathcal{N}_i^k(X)} \alpha_X [Q(\mathbf{f}_i, \vec{x}_i)K(\mathbf{f}_j, \vec{x}_j, \vec{x}_i)] W_V(\vec{x}_j - \vec{x}_i)\mathbf{f}_j \\
&= \rho_{\text{out}}(r) \text{SA}[\mathbf{F}(X), X]_i.
\end{aligned}$$

Thus each self-attention layer in  $\mathcal{F}$  is equivariant. The same holds for each cross-attention layer in  $\mathcal{T}$ , except that if the closest neighbor of the query is not uniquely defined, then—as discussed above—we output the entire set of fields for every equivalent neighborhood. Then, the output is also a set of fields and a roto-translation of the input will only result in a permutation of these fields. Then, the “max” operation in the output will eliminate the permutation, making the output equivariant.

In the first step above, we proved the base case of the induction argument—in the number of layers—namely that the input to each attention module at the first layer transforms as a field. In the second step we proved the inductive step, namely that given a  $\rho_{\text{in}}$ -field in the input, an attention layer produces a  $\rho_{\text{out}}$ -field in the output. Thus, by induction on the number of layers, a composition of multiple self-attention layers outputs an equivariant field. We select a type-0 field for the output of our network, in accordance with the properties of an occupancy field. Then, by definition, the field transforms according to the trivial representation of  $\text{SO}(3)$ , i.e.,  $\rho_{\text{out}}(r) = I$ .

Thus the map

$$(X, \vec{q}) \rightarrow \mathcal{T}(\mathcal{F}[S_1(X), X], X, S_2(X, \vec{q}), \vec{q})$$

is  $(\text{SE}(3), \mathcal{L}_{\text{in}}, \mathcal{L}_{\text{out}})$ -equivariant, with  $\mathcal{L}_{\text{in}}$  being the direct sum of  $N + 1$  standard representations of  $\text{SE}(3)$ , as analyzed in Step 1, and  $\mathcal{L}_{\text{out}}$  is the trivial representation of  $\text{SE}(3)$ . In other words, viewed as a function on  $(X, \vec{q})$ ,  $\mathcal{T}$  is a scalar field satisfying

$$\mathcal{T}[\mathcal{L}_{\text{in}(t,r)}[X, \vec{q}]] = \mathcal{T}[X, \vec{q}].$$

**Additional Equivariant Layers:** Clearly, the concatenation of *multiple attention heads* with the same irreducible types, as well as *skip connection* layers as defined in section 6.5, preserve equivariance. Since they add the multiplicities of each irreducible type independently, they only change the output representation by increasing the multiplicities of its irreducibles.

The subsequent mixing of channels of the same irreducible type by a linear map performed in the multi-head attention module corresponds to the same operation that the query performs, thus it also preserves equivariance.

Finally, the equivariant layer-norm layer also operates on each irreducible type independently. Since the irreducibles are unitary transforms—i.e.,  $\|\mathbf{f}_{l,m_l}\|_2 = \|\mathbf{D}_l \mathbf{f}_{l,m_l}\|_2$  for all  $\mathbf{f}_{l,m_l}$  and all  $\mathbf{D}_l$ —any non-linear operation on the norm of a *type-l* vector produces a *type-0* vector. Since  $\mathbf{f}_{l,m_l} / \|\mathbf{f}_{l,m_l}\|_2$  is again a *type-l* vector, the final result is a *type-l* vector.

**Attention as a set operation:** In addition to  $\text{SE}(3)$ -equivariance, our model inherits the properties of the standard attention layers. Thus, it is equivariant to any permutation of the points in the point cloud, and to the order of the queries. Moreover, the number of output tokens can vary. We use this property for scene reconstruction, e.g., in Section 6.1 by reconstructing scenes of a variable number of points (and point clouds) even by training on single objects of a fixed number of points. The input (key-value) tokens can also change during inference, which we can use to adapt the neighborhoods dynamically during inference. This can counter that super-sampling a point cloud may reduce the receptive field.

**On independent  $\text{SO}(3)$  rotations.** Our local attention neighborhoods and equivariant reconstructions are particularly important properties when reconstructing scenes. Here the point clouds can be independently placed in arbitrary positions. It is natural to ask if we can connect the performance of our model in a particular scene to the performance in another scene, where the same point

clouds have been independently roto-translated. For a single object, the true occupancy function should be the same under a simultaneous roto-translation of the point cloud and the query. Our equivariant pipeline respects this property, by outputting a scalar field. Thus, the performance of our model is consistent independently of the  $SE(3)$  transformations of a single point cloud.

Following a similar approach for scenes with multiple objects, one can associate an independent copy of  $SO(3)$  acting on each point cloud, i.e., an action  $X^i \mapsto \mathcal{L}_{r_i}[X^i]$ , for all objects  $i \in I$ . We can ask if there is a transformation of the query  $\vec{q}$ , that, after the rotation of the point clouds, results in the same occupancy value. Also, can this be implemented without knowing the segmentation function that assigns the points to their point clouds? A reasonable first approach would be to transform the query  $\vec{q}$  with the rotation matrix  $R_i$  used to transform its closest neighbor.

Unfortunately, this transformation does not correspond to a group action. To understand this, consider two unit spheres at positions  $(0, 0, 0)$  and  $(1, 0, 0)$  in three-dimensional space, and the query point  $\vec{q} = (-10, 0, 0)$ . Then, consider the product group action  $\mathcal{L}_1 = \mathcal{L}_{r_1, r_2} = \mathcal{L}_{(0, 0, \pi), e}$  that rotates the first sphere around the  $z$ -axis by 180 degrees— $r_1 = (0, 0, \pi)$ —and fixes the second sphere— $r_2 = e$ . Next, consider the reverse action  $\mathcal{L}_2 = \mathcal{L}_{(0, 0, -\pi), e}$ . If we first multiply the corresponding group elements together, we find  $\mathcal{L} = \mathcal{L}_1 \circ \mathcal{L}_2 = \mathcal{L}_{e, e} = I$ . If we then find the nearest sphere and apply the identity action to the query, it will remain at  $(-10, 0, 0)$ . On the other hand, if we first find the nearest neighbor—in this case, the first sphere—and apply the corresponding action, then the query will rotate around the  $z$ -axis by 180-degrees, moving to  $(10, 0, 0)$ . If we then apply the second action by finding again the nearest neighbor—now the second sphere—the identity action will be applied and the query point stays at  $(10, 0, 0)$ . Thus, this transformation does not satisfy the “compatibility” property and thus it is not a group action.

Even though the conditions are not met for all query points in space, there are subsets of  $\mathbb{R}^3$  that are closed under these transformations and for which these transformations indeed form group actions. We will consider equivariance only in those subsets. We construct them geometrically for two point clouds for simplicity. Consider the point clouds  $X_1, X_2$  rotating around points  $c_1, c_2$ , respectively. We construct the equivariant zone for the point cloud  $X_1$ . First take the point in  $X_2$  that has the maximum distance (in Euclidean norm), say  $d_2$ , to its center of rotation  $c_2$ . Form the sphere  $S_2$  around  $X_2$ , with a radius  $d_2$  and center  $c_2$ . All of  $X_2$  is contained in  $S_2$ . Connect the centers  $c_1, c_2$ , and denote the point of intersection of this segment with  $S_2$  as  $p$ . Then, draw the segment between  $p$  and  $c_1$  and name the distance of  $c_1$  to the middle point of this segment  $D_1$ . Every point in the sphere  $S_1$  of radius  $D_1$  and center  $c_1$  is in the equivariant zone of  $X_1$ , called  $Z_1$ .

We prove that in the equivariant zone, our model is equivariant, for any independent rotation of the point clouds. By construction, every query  $\vec{q}$  in the first equivariant zone  $Z_1$  has its closest neighbor in the point cloud  $X_1$ . This holds for any rotation of any point cloud. Then, by definition, the action on the

query is the same rotation  $R_{r_1}$  that transformed the points in  $X_1$ . Since the point cloud and the query both rotate with the same transformation, the query neighborhood constructed within the cross-attention layers is invariant—leading to the same closest neighbor—as we proved for the single object case.

Now, suppose each point in  $X_1$  has its  $k$  nearest neighbors in  $X_1$ , for any rotation of the point clouds; this is reasonable for sufficiently dense or separated point clouds. Then these point cloud neighborhoods are also invariant after the individual rotations. Under these conditions, a direct product action of  $\text{SO}(3)$ -s on the point clouds with a simultaneous action of  $R_1$  on the query in the first equivariant zone is viewed by the attention network as a simultaneous rotation of the point cloud  $X_1$  and the query  $\vec{q}$ . This is because  $\mathcal{N}(\vec{q})$  contains only points from  $X_1$ , so the attention module uses only key-value tokens from points in  $X_1$ . Further, the neighborhood of the query is invariant to a simultaneous rotation of  $X_1$  and  $\vec{q}$ . Thus, as we proved in the single-object case, the occupancy value prediction for this transformed query is invariant to the transformation. Thus, for all queries in an equivariant zone, equivariance to the direct product action of  $\text{SO}(3)$  holds, i.e., for all  $r_1, r_2, \dots, r_I \in \text{SO}(3)$ , and for all  $\vec{q} \in Z_j$ , with  $j \in [I]$

$$\mathcal{T}[(\mathcal{L}_{r_1}[X_1], \mathcal{L}_{r_2}[X_2], \dots, \mathcal{L}_{r_I}[X_I]), R_j \vec{q}] = \mathcal{T}[(X_1, X_2, \dots, X_I), \vec{q}].$$

## References

1. Alexa, M., Behr, J., Cohen-Or, D., Fleishman, S., Levin, D., Silva, C.: Computing and rendering point set surfaces. *IEEE Transactions on Visualization and Computer Graphics* **9**(1), 3–15 (2003). <https://doi.org/10.1109/TVCG.2003.1175093>
2. Ba, J.L., Kiros, J.R., Hinton, G.E.: Layer normalization. *arXiv preprint arXiv:1607.06450* (2016)
3. Bahdanau, D., Cho, K., Bengio, Y.: Neural machine translation by jointly learning to align and translate. In: Bengio, Y., LeCun, Y. (eds.) *3rd International Conference on Learning Representations, ICLR 2015, San Diego, CA, USA, May 7-9, 2015, Conference Track Proceedings (2015)*, <http://arxiv.org/abs/1409.0473>
4. Berger, M., Tagliasacchi, A., Seversky, L.M., Alliez, P., Guennebaud, G., Levine, J.A., Sharf, A., Silva, C.T.: A survey of surface reconstruction from point clouds. In: *Computer Graphics Forum*. vol. 36, pp. 301–329. Wiley Online Library (2017)
5. Chabra, R., Lenssen, J.E., Ilg, E., Schmidt, T., Straub, J., Lovegrove, S., Newcombe, R.: Deep local shapes: Learning local sdf priors for detailed 3d reconstruction. In: *ECCV 2020: 16th European Conference*. p. 608–625 (2020)
6. Chang, A., Dai, A., Funkhouser, T., Halber, M., Niessner, M., Savva, M., Song, S., Zeng, A., Zhang, Y.: Matterport3d: Learning from rgb-d data in indoor environments. *International Conference on 3D Vision (3DV)* (2017)
7. Chang, A.X., Funkhouser, T., Guibas, L., Hanrahan, P., Huang, Q., Li, Z., Savarese, S., Savva, M., Song, S., Su, H., Xiao, J., Yi, L., Yu, F.: ShapeNet: An Information-Rich 3D Model Repository. Tech. Rep. arXiv:1512.03012 [cs.GR], Stanford University — Princeton University — Toyota Technological Institute at Chicago (2015)
8. Chen, H., Liu, S., Chen, W., Li, H., Hill, R.: Equivariant point network for 3d point cloud analysis. In: *Proceedings of the IEEE/CVF Conference on Computer Vision and Pattern Recognition*. pp. 14514–14523 (2021)

9. Chen, Z., Zhang, H.: Learning implicit fields for generative shape modeling. In: Proceedings of the IEEE/CVF Conference on Computer Vision and Pattern Recognition. pp. 5939–5948 (2019)
10. Chen, Z., Zhang, H.: Learning implicit fields for generative shape modeling. In: Proceedings of the IEEE/CVF Conference on Computer Vision and Pattern Recognition (CVPR) (June 2019)
11. Choy, C.B., Xu, D., Gwak, J., Chen, K., Savarese, S.: 3d-r2n2: A unified approach for single and multi-view 3d object reconstruction. In: Proceedings of the European Conference on Computer Vision (ECCV) (2016)
12. Cohen, T., Weiler, M., Kicanaoglu, B., Welling, M.: Gauge equivariant convolutional networks and the icosahedral CNN. In: Proceedings of the 36th International Conference on Machine Learning. vol. 97, pp. 1321–1330 (2019)
13. Cohen, T., Welling, M.: Group equivariant convolutional networks. In: International conference on machine learning. pp. 2990–2999 (2016)
14. Deng, C., Litany, O., Duan, Y., Poulencard, A., Tagliasacchi, A., Guibas, L.: Vector neurons: a general framework for  $so(3)$ -equivariant networks. arXiv preprint arXiv:2104.12229 (2021)
15. Deng, C., Litany, O., Duan, Y., Poulencard, A., Tagliasacchi, A., Guibas, L.J.: Vector neurons: A general framework for  $so(3)$ -equivariant networks. In: Proceedings of the IEEE/CVF International Conference on Computer Vision (ICCV). pp. 12200–12209 (October 2021)
16. Dosovitskiy, A., Beyer, L., Kolesnikov, A., Weissenborn, D., Zhai, X., Unterthiner, T., Dehghani, M., Minderer, M., Heigold, G., Gelly, S., Uszkoreit, J., Houlsby, N.: An image is worth 16x16 words: Transformers for image recognition at scale. In: International Conference on Learning Representations (2021), <https://openreview.net/forum?id=YicbFdNTTy>
17. Erler, P., Guerrero, P., Ohrhallinger, S., Mitra, N.J., Wimmer, M.: Points2Surf: Learning implicit surfaces from point clouds. In: Vedaldi, A., Bischof, H., Brox, T., Frahm, J.M. (eds.) Computer Vision – ECCV 2020. pp. 108–124. Springer International Publishing, Cham (2020)
18. Esteves, C., Allen-Blanchette, C., Makadia, A., Daniilidis, K.: Learning  $so(3)$  equivariant representations with spherical cnns. In: The European Conference on Computer Vision (ECCV) (September 2018)
19. Fan, H., Su, H., Guibas, L.J.: A point set generation network for 3d object reconstruction from a single image. In: Proceedings of the IEEE Conference on Computer Vision and Pattern Recognition (CVPR) (July 2017)
20. Fuchs, F.B., Worrall, D.E., Fischer, V., Welling, M.:  $Se(3)$ -transformers: 3d rotation equivariant attention networks. In: Advances in Neural Information Processing Systems 34 (NeurIPS) (2020)
21. Fukushima, K.: Neocognitron: A self-organizing neural network model for a mechanism of pattern recognition unaffected by shift in position. *Biological cybernetics* **36**(4), 193–202 (1980)
22. Fulton, W., Harris, J.: Representation theory: a first course, vol. 129. Springer Science & Business Media (2013)
23. Genova, K., Cole, F., Sud, A., Sarna, A., Funkhouser, T.: Local deep implicit functions for 3d shape. In: The IEEE Conference on Computer Vision and Pattern Recognition (CVPR). pp. 4856–4865 (06 2020). <https://doi.org/10.1109/CVPR42600.2020.00491>
24. Gong, S., Chen, L., Bronstein, M., Zafeiriou, S.: Spiralnet++: A fast and highly efficient mesh convolution operator. In: Proceedings of the IEEE/CVF International Conference on Computer Vision Workshops. pp. 0–0 (2019)



25. Hall, B.C., et al.: Lie groups, Lie algebras, and representations: an elementary introduction, vol. 10. Springer (2003)
26. Jiang, C.M., Sud, A., Makadia, A., Huang, J., Nießner, M., Funkhouser, T.: Local implicit grid representations for 3d scenes. In: Proceedings IEEE Conf. on Computer Vision and Pattern Recognition (CVPR) (2020)
27. Kazhdan, M., Hoppe, H.: Screened poisson surface reconstruction. *ACM Trans. Graph.* **32**(3) (jul 2013). <https://doi.org/10.1145/2487228.2487237>, <https://doi.org/10.1145/2487228.2487237>
28. Kendall, D.G.: A survey of the statistical theory of shape. *Statistical Science* **4**(2), 87–99 (1989)
29. Kingma, D.P., Ba, J.: Adam: A method for stochastic optimization. In: 3rd International Conference on Learning Representations, ICLR 2015, San Diego, CA, USA, May 7-9, 2015, Conference Track Proceedings (2015)
30. LeCun, Y., Boser, B., Denker, J.S., Henderson, D., Howard, R.E., Hubbard, W., Jackel, L.D.: Backpropagation applied to handwritten zip code recognition. *Neural computation* **1**(4), 541–551 (1989)
31. Lionar, S., Emtsev, D., Svilarkovic, D., Peng, S.: Dynamic plane convolutional occupancy networks. In: Winter Conference on Applications of Computer Vision (WACV) (2021)
32. Lorensen, W.E., Cline, H.E.: Marching cubes: A high resolution 3d surface construction algorithm. In: Proceedings of the 14th Annual Conference on Computer Graphics and Interactive Techniques. p. 163–169. SIGGRAPH '87, Association for Computing Machinery, New York, NY, USA (1987)
33. Lorensen, W.E., Cline, H.E.: Marching cubes: A high resolution 3d surface construction algorithm. *ACM siggraph computer graphics* **21**(4), 163–169 (1987)
34. Maron, H., Ben-Hamu, H., Shamir, N., Lipman, Y.: Invariant and equivariant graph networks. In: 7th International Conference on Learning Representations, ICLR 2019, New Orleans, LA, USA, May 6-9, 2019 (2019)
35. Mescheder, L., Oechsle, M., Niemeyer, M., Nowozin, S., Geiger, A.: Occupancy networks: Learning 3d reconstruction in function space. In: Proceedings IEEE Conf. on Computer Vision and Pattern Recognition (CVPR) (2019)
36. Niemeyer, M., Geiger, A.: Giraffe: Representing scenes as compositional generative neural feature fields. In: Proceedings of the IEEE/CVF Conference on Computer Vision and Pattern Recognition. pp. 11453–11464 (2021)
37. Niemeyer, M., Mescheder, L., Oechsle, M., Geiger, A.: Differentiable volumetric rendering: Learning implicit 3d representations without 3d supervision. In: Proceedings of the IEEE/CVF Conference on Computer Vision and Pattern Recognition. pp. 3504–3515 (2020)
38. Pan, X., Xia, Z., Song, S., Li, L.E., Huang, G.: 3d object detection with pointformer. In: Proceedings of the IEEE/CVF Conference on Computer Vision and Pattern Recognition (CVPR). pp. 7463–7472 (June 2021)
39. Park, J.J., Florence, P., Straub, J., Newcombe, R., Lovegrove, S.: Deepsdf: Learning continuous signed distance functions for shape representation. In: The IEEE Conference on Computer Vision and Pattern Recognition (CVPR) (June 2019)
40. Peng, S., Niemeyer, M., Mescheder, L., Pollefeys, M., Geiger, A.: Convolutional occupancy networks. In: European Conference on Computer Vision. pp. 523–540. Springer (2020)
41. Poulénard, A., Guibas, L.J.: A functional approach to rotation equivariant nonlinearities for tensor field networks. In: Proceedings of the IEEE/CVF Conference on Computer Vision and Pattern Recognition (CVPR). pp. 13174–13183 (June 2021)

42. Qi, C.R., Su, H., Mo, K., Guibas, L.J.: Pointnet: Deep learning on point sets for 3d classification and segmentation (2016), <http://arxiv.org/abs/1612.00593>, cite arxiv:1612.00593
43. Riegler, G., Osman Ulusoy, A., Geiger, A.: Octnet: Learning deep 3d representations at high resolutions. In: Proceedings of the IEEE conference on computer vision and pattern recognition. pp. 3577–3586 (2017)
44. Romero, D.W., Cordonnier, J.B.: Group equivariant stand-alone self-attention for vision. In: International Conference on Learning Representations (2021), <https://openreview.net/forum?id=JkfYjn0Eo6M>
45. Sitzmann, V., Zollhöfer, M., Wetzstein, G.: Scene representation networks: Continuous 3d-structure-aware neural scene representations. *Advances in Neural Information Processing Systems* **32** (2019)
46. Tang, J., Lei, J., Xu, D., Ma, F., Jia, K., Zhang, L.: Sa-convonet: Sign-agnostic optimization of convolutional occupancy networks. In: Proceedings of the IEEE/CVF International Conference on Computer Vision (2021)
47. Tatarchenko, M., Richter, S.R., Ranftl, R., Li, Z., Koltun, V., Brox, T.: What do single-view 3d reconstruction networks learn? In: Proceedings of the IEEE/CVF Conference on Computer Vision and Pattern Recognition (CVPR) (June 2019)
48. Thomas, N., Smidt, T., Kearnes, S., Yang, L., Li, L., Kohlhoff, K., Riley, P.: Tensor field networks: Rotation-and translation-equivariant neural networks for 3d point clouds. arXiv preprint arXiv:1802.08219 (2018)
49. Tretschk, E., Tewari, A., Golyanik, V., Zollhöfer, M., Stoll, C., Theobalt, C.: PatchNets: Patch-Based Generalizable Deep Implicit 3D Shape Representations. *European Conference on Computer Vision (ECCV)* (2020)
50. Vaswani, A., Shazeer, N., Parmar, N., Uszkoreit, J., Jones, L., Gomez, A.N., Kaiser, L.u., Polosukhin, I.: Attention is all you need. In: Guyon, I., Luxburg, U.V., Bengio, S., Wallach, H., Fergus, R., Vishwanathan, S., Garnett, R. (eds.) *Advances in Neural Information Processing Systems*. vol. 30. Curran Associates, Inc. (2017)
51. Wang, H., Zhang, J.: A survey of deep learning-based mesh processing. *Communications in Mathematics and Statistics* pp. 1–32 (2022)
52. Weiler, M., Geiger, M., Welling, M., Boomsma, W., Cohen, T.: 3d steerable cnns: Learning rotationally equivariant features in volumetric data. In: *NeurIPS* (2018)
53. Weiler, M., Hamprecht, F.A., Storath, M.: Learning steerable filters for rotation equivariant cnns. In: *2018 IEEE Conference on Computer Vision and Pattern Recognition, CVPR 2018, Salt Lake City, UT, USA, June 18–22, 2018*. pp. 849–858. IEEE Computer Society (2018)
54. Wu, H., Xiao, B., Codella, N., Liu, M., Dai, X., Yuan, L., Zhang, L.: Cvt: Introducing convolutions to vision transformers. In: *Proceedings of the IEEE/CVF International Conference on Computer Vision (ICCV)*. pp. 22–31 (October 2021)
55. Yu, X., Rao, Y., Wang, Z., Liu, Z., Lu, J., Zhou, J.: Pointr: Diverse point cloud completion with geometry-aware transformers. In: *ICCV* (2021)